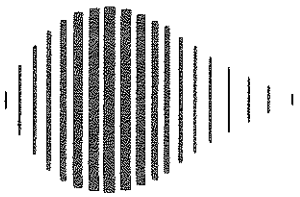

NATIONAL CENTER FOR EARTHQUAKE
ENGINEERING RESEARCH
State University of New York at Buffalo

DIGITAL SIMULATION OF SEISMIC GROUND MOTION

by

M. Shinozuka, G. Deodatis and T. Harada
Department of Civil Engineering and
Engineering Mechanics
Columbia University
New York, NY 10027-6699

Technical Report NCEER-87-0017

August 31, 1987

This research was conducted at Columbia University and was partially supported by the National Science Foundation under Grant No. ECE 86-07591

NOTICE

This report was prepared by Columbia University as a result of research sponsored by the National Center for Earthquake Engineering Research (NCEER). Neither NCEER, associates of NCEER, its sponsors, Columbia University, nor any person acting on their behalf:

a. makes any warranty, express or implied, with respect to the use of any information, apparatus, method, or process disclosed in this report or that such use may not infringe upon privately owned rights; or

b. assumes any liabilities of whatsoever kind with respect to the use of, or for damages resulting from the use of, any information, apparatus, method or process disclosed in this report.

DIGITAL SIMULATION OF SEISMIC GROUND MOTION*

by

M. Shinozuka[1], G. Deodatis[2] and T. Harada[3]

August 31, 1987

Technical Report NCEER-87-0017

NCEER Contract Number 86-3043

NSF Master Contract Number ECE-86-07591

1 Renwick Professor, Dept. of Civil Engineering and Engineering Mechanics, Columbia University
2 Post-Doctoral Research Scientist, Dept. of Civil Engineering and Engineering Mechanics, Columbia University
3 Associate Professor, Dept. of Civil Engineering, Miyazaki University, Japan

NATIONAL CENTER FOR EARTHQUAKE ENGINEERING RESEARCH
State University of New York at Buffalo
Red Jacket Quadrangle, Buffalo, NY 14261

---

* Slightly revised version of paper under same title presented at US-Japan Joint Seminar on Stochastic Approaches in Earthquake Engineering, Florida Atlantic University, Boca Raton, Florida, May 6-7, 1987.

SUMMARY

The method of spectral representation for uni-variate, one-dimensional, stationary stochastic processes and multi-dimensional, uni-variate (as well as multi-dimensional, multi-variate) homogeneous stochastic fields has been reviewed, particularly from the viewpoint of digitally generating their sample functions. This method of representation has then been extended to the cases of uni-variate, one-dimensional, nonstationary stochastic processes and multi-dimensional, uni-variate nonhomogeneous stochastic fields, again emphasizing sample function generation. Also, a fundamental theory of evolutionary stochastic waves is developed and a technique for digitally generating samples of such waves is introduced as a further extension of the spectral representation method. This is done primarily for the purpose of developing an analytical model of seismic waves that can account for their stochastic characteristics in the time and space domain. From this model, the corresponding sample seismic waves can be digitally generated. The efficacy of this new technique is demonstrated with the aid of a numerical example in which a sample of a spatially two-dimensional stochastic wave consistent with the Lotung, Taiwan dense array data is digitally generated.

KEYWORDS

Simulation; ground motion; spectral representation; stochastic process; stochastic field; stochastic wave; stationarity; nonstationarity; homogeneity; nonhomogeneity; power specrum; evolutionary power spectrum; autocorrelation function.

TABLE OF CONTENTS

SECTION	TITLE	PAGE
1	INTRODUCTION	1-1
2	SIMULATION OF SEISMIC GROUND MOTION USING STATIONARY PROCESS AND HOMOGENEOUS FIELD MODELS	2-1
2.1	Simulation of 1D-1V Stationary Stochastic Processes Using Spectral Representation	2-1
2.2	Simulation of nD-1V Homogeneous Stochastic Fields Using Spectral Representation	2-5
2.3	Simulation of nD-mV Homogeneous Stochastic Fields Using Spectral Representation	2-10
3	SIMULATION OF SEISMIC GROUND MOTION USING NON-STATIONARY PROCESS AND NON-HOMOGENEOUS FIELD MODELS	3-1
3.1	Simulation of 1D-1V Nonstationary Stochastic Processes Using Spectral Representation	3-1
3.2	Simulation of nD-1V Nonhomogeneous Stochastic Fields Using Spectral Representation	3-3
4	SIMULATION OF SEISMIC GROUND MOTION USING STOCHASTIC WAVES	4-1
4.1	Theory of nD-1V Stochastic Waves	4-1
4.2	Application to Spatially One-Dimensional Stochastic Waves	4-5
4.3	Numerical Example Involving a Non-Stationary Stochastic Wave With Two-Dimensional Spatial Nonhomogeneity	4-8
5	CONCLUSION	5-1
	ACKNOWLEDGEMENT	5-3
6	REFERENCES	6-1

LIST OF ILLUSTRATIONS

FIGURE	TITLE	PAGE
1	Function B	4-13
2	Function W	4-14
3	Power Spectrum f	4-15
4a-d	Simulated Stochastic Wave at 12 Equispaced Time Instants	4-16
5	Time History of Displacement at the Four Points A, B, C and D shown in Fig. 4a	4-20

1. INTRODUCTION

A number of stochastic models for the digital generation of artificial ground acceleration have been proposed and successfully applied to a variety of structural problems arising from seismic events. Referring only to representative earlier work in this area, the following papers are cited: those by Tajimi[1], Cornell[2], Housner and Jennings[3], Shinozuka and Sato[4], Amin and Ang[5], Iyengar and Iyengar[6], Ruiz and Penzien[7] and Lin[8]. Later on, Shinozuka and his associates introduced in a series of papers [9-14] the spectral representation method, which can be easily implemented for the digital simulation of ground accelerations or displacements. The papers by Shinozuka and his associates clearly recognized the multi-variate and multi-dimensional nature of ground motion. The most recent development in this field is the use of Auto-Regressive Moving-Average (ARMA) models which have been studied by Shinozuka and his associates[15-19], Spanos and his associates[20-22] and Kozin and Nakajima[23].

A common limitation of all the above models is that ground motion is treated as a stochastic process when its time variability is examined, or as a stochastic field when its spatial variability is considered. In the former case, the space variables are frozen, while in the latter case, time is frozen. In order to have the analysis reflect the obvious nature of ground motion arising from a propagating seismic wave, a stochastic wave model with evolutionary power has been developed here and an efficient technique for digitally generating samples of such a stochastic wave is introduced as an extension of the spectral representation method primarily developed by Shinozuka and his associates. Such a model is useful for the seismic response analysis of such large-scale structures extending over a wide spatial area as water transmission and gas distribution systems and large-span bridges.

2. SIMULATION OF SEISMIC GROUND MOTION USING STATIONARY PROCESS AND HOMOGENEOUS FIELD MODELS

2.1 Simulation of 1D-1V Stationary Stochastic Processes Using Spectral Representation

Considerable progress has been made in stochastic modeling of ground motion and in generating the corresponding sample functions for the purpose of nonlinear and/or parametric seismic response analyses. However, a large number of these analyses are still performed under the assumption that seismic ground motion consists of a single horizontal component. In this respect, the digital simulation of 1D-1V (one-dimensional and uni-variate) stationary stochastic processes using spectral representation[14] remains of critical importance in the seismic response analysis of structures.

Let $f_0(t)$ be a 1D-1V stationary stochastic process with mean zero and auto-correlation function $R_{f_0f_0}(\tau)$. Then

$$E[f_0(t)] = 0 \tag{1}$$

$$E[f_0(t+\tau)f_0(t)] = R_{f_0f_0}(\tau) \tag{2}$$

where $E[\cdot]$ indicates the expectation. It is well known that $R_{f_0f_0}(\tau)$ and the power spectral density function $S_{f_0f_0}(\omega)$ of the process $f_0(t)$ are related through the Weiner-Khintchine transform pair:

$$S_{f_0f_0}(\omega) = \frac{1}{2\pi}\int_{-\infty}^{\infty} R_{f_0f_0}(\tau)e^{-i\omega\tau}d\tau \tag{3}$$

$$R_{f_0f_0}(\tau) = \int_{-\infty}^{\infty} S_{f_0f_0}(\omega)e^{i\omega\tau}d\omega \tag{4}$$

It follows immediately from Eq. 2 that $R_{f_0f_0}(\tau)$ is an even function of τ, and consequently the power spectral density $S_{f_0f_0}(\omega)$ is also an even function of ω in accordance with Eq. 3. Also, it can be shown that $S_{f_0f_0}(\omega) \geq 0$.

It will be shown that the stochastic process $f_0(t)$ can be simulated by

the following series, as $N \to \infty$.

$$f(t) = \sqrt{2} \sum_{j=1}^{N} \sqrt{2S_{f_0 f_0}(\omega_j)\Delta\omega} \cdot \cos(\omega_j t + \phi_j) \tag{5}$$

where

$$\omega_j = j\Delta\omega \qquad j=1,2,\ldots,N \tag{6}$$

An upper bound of the frequency

$$\omega_u = N\Delta\omega \tag{7}$$

is implicit in Eq. 5 where ω_u represents an upper cut-off frequency beyond which $S_{f_0 f_0}(\omega)$ may be assumed to be zero for either mathematical or physical reasons. In Eq. 5, ϕ_j are independent random phase angles uniformly distributed over the range $(0,2\pi)$. Note that the simulated process is asymptotically Gaussian as N becomes large due to the central limit theorem.

It will be shown now that the expected value and auto-correlation function of the simulated process f(t) are identical to the corresponding targets, $E[f_0(t)] = 0$ and $R_{f_0 f_0}(\tau)$, respectively. First, utilizing the assumption that the random phase angles are independent, the expected value E[f(t)] becomes:

$$E[f(t)] = \sqrt{2} \int_{-\infty}^{\infty} \overset{\text{N-fold}}{\cdots\cdots} \int_{-\infty}^{\infty} \sum_{j=1}^{N} \sqrt{2S_{f_0 f_0}(\omega_j)\Delta\omega} \cdot \cos(\omega_j t+\phi_j) \cdot \prod_{i=1}^{N} [p_{\Phi_i}(\phi_i)d\phi_i] \tag{8}$$

where $p_{\Phi_i}(\cdot)$ is the density function of Φ_i and hence:

$$p_{\Phi_i}(\phi_i) = \begin{cases} \frac{1}{2\pi} & 0 \leq \phi_i \leq 2\pi \\ 0 & \text{otherwise} \end{cases} \tag{9}$$

The N-fold integral appearing in Eq. 8 can be written as follows:

$$\int_{-\infty}^{\infty} \overset{N\text{-fold}}{\cdots\cdots} \int_{-\infty}^{\infty} \cos(\omega_j t + \phi_j) \prod_{i=1}^{N} [p_{\Phi_i}(\phi_i) d\phi_i]$$

$$= \prod_{\substack{i=1 \\ i\neq j}}^{N} \{\int_{-\infty}^{\infty} p_{\Phi_i}(\phi_i) d\phi_i\} \int_{-\infty}^{\infty} \cos(\omega_j t + \phi_j) p_{\Phi_j}(\phi_j) d\phi_j$$

$$= \int_0^{2\pi} \frac{1}{2\pi} \cos(\omega_j t + \phi_j) d\phi_j = \frac{1}{2\pi} \cdot [\sin(\omega_j t + \phi_j)]_0^{2\pi} = 0 \qquad (10)$$

It has therefore been shown that:

$$E[f(t)] = 0 \qquad (11)$$

Second, the auto-correlation function of the simulated process f(t) is calculated as follows:

$$R_{ff}(\tau) = E[f(t+\tau)f(t)] =$$

$$= \int_{-\infty}^{\infty} \overset{N\text{-fold}}{\cdots\cdots} \int_{-\infty}^{\infty} 2 \sum_{i=1}^{N} \sum_{j=1}^{N} \sqrt{2S_{f_0 f_0}(\omega_i)\Delta\omega} \sqrt{2S_{f_0 f_0}(\omega_j)\Delta\omega} \cdot$$

$$\cos[\omega_i(t+\tau) + \phi_i] \cdot \cos[\omega_j t + \phi_j] \cdot \prod_{\ell=1}^{N} [p_{\Phi_\ell}(\phi_\ell) d\phi_\ell] \qquad (12)$$

The following double integral is needed in the derivation of the expression of $R_{ff}(\tau)$:

$$\int_{-\infty}^{\infty} \int_{-\infty}^{\infty} \cos[\omega_i(t+\tau) + \phi_i] \cdot \cos[\omega_j t + \phi_j] \cdot p_{\Phi_i}(\phi_i) \cdot p_{\Phi_j}(\phi_j) d\phi_i d\phi_j =$$

$$= \frac{1}{2} \int_{-\infty}^{\infty} \int_{-\infty}^{\infty} [\cos\{(\omega_i+\omega_j)t + \omega_i\tau + \phi_i + \phi_j\} +$$

$$+ \cos\{(\omega_i-\omega_j)t + \omega_i\tau + \phi_i - \phi_j\}] \cdot p_{\Phi_i}(\phi_i) \cdot p_{\Phi_j}(\phi_j) d\phi_i d\phi_j \qquad (13)$$

The expression for the double integral appearing in Eq. 13 is equal to zero when $i \neq j$. It is different from zero only when $i = j$;

$$\int_{-\infty}^{\infty} \cos[\omega_i(t+\tau) + \phi_i] \cdot \cos[\omega_i t + \phi_i] \cdot p_{\Phi_i}(\phi_i)d\phi_i =$$

$$= \frac{1}{2}\int_{-\infty}^{\infty} [\cos(2\omega_i t + \omega_i \tau + 2\phi_i) + \cos(\omega_i \tau)] \cdot p_{\Phi_i}(\phi_i)d\phi_i =$$

$$= \frac{1}{2} \cdot \cos(\omega_i \tau) \tag{14}$$

Using Eqs. 13 and 14, Eq. 12 eventually yields the following expression for $R_{ff}(\tau)$:

$$R_{ff}(\tau) = E[f(t+\tau)f(t)] = \sum_{i=1}^{N} 2S_{f_0f_0}(\omega_i)\Delta\omega \cdot \cos(\omega_i \tau) \tag{15}$$

If, in Eq. 15, the limit is taken as $N \to \infty$, while keeping $\omega_u = N\Delta\omega$ constant and remembering that $S_{f_0f_0}(\omega) = 0$ for $|\omega| \geq \omega_u$, it follows that

$$R_{ff}(\tau) = 2\int_0^{\infty} S_{f_0f_0}(\omega) \cos(\omega\tau)d\omega = \int_{-\infty}^{\infty} S_{f_0f_0}(\omega)e^{i\omega\tau}\, d\omega \tag{16}$$

Then, by virtue of Eq. 4:

$$R_{ff}(\tau) = R_{f_0f_0}(\tau) \tag{17}$$

It has therefore been shown that the expected value and autocorrelation function of the simulated process are the same with the target ones, i.e., $E[f(t)] = E[f_0(t)] = 0$ and $R_{ff}(\tau) = R_{f_0f_0}(\tau)$.

At this juncture, it must be noted that the simulated process given by Eq. 5 is ergodic, at least to the second moment, regardless of the size of

N [14]. This makes the method directly applicable to time-domain analysis in which the ensemble average can be evaluated in terms of the temporal average. Finally, it should be pointed out that the computer cost of the digital generation of sample functions of process f(t) can be dramatically reduced by applying the FFT (Fast Fourier Transform) technique to Eq. 5 [13].

2.2 Simulation of nD-1V Homogeneous Stochastic Fields Using Spectral Representation

The simulation of 1D-1V stationary stochastic processes using spectral representation, which was presented in the previous section, can be extended in a straightforward fashion to the simulation of nD-1V (n-dimensional and uni-variate) homogeneous stochastic fields[14] in the following way.

Consider an nD-1V homogeneous stochastic field $f_0(x_1, x_2, \ldots, x_n) = f_0(\underline{x})$ with mean zero:

$$E[f_0(\underline{x})] = 0 \tag{18}$$

The autocorrelation function of $f_0(\underline{x})$ is defined by

$$R_{f_0 f_0}(\underline{\xi}) = E[f_0(\underline{x}_r) f_0(\underline{x}_s)] \tag{19}$$

where $\underline{x}_r$ and $\underline{x}_s$ are position vectors in an n-dimensional space and $\underline{\xi}$ is the separation vector. For a homogeneous field, $R_{f_0 f_0}(\underline{\xi})$ is symmetric with respect to the separation vector $\underline{\xi}$ and therefore:

$$R_{f_0 f_0}(\underline{\xi}) = R_{f_0 f_0}(-\underline{\xi}) \tag{20}$$

For some nD-1V homogeneous fields, the following equation is valid:

$$R_{f_0 f_0}(\underline{\xi}) = R_{f_0 f_0}(I_{\pm}\,\underline{\xi}) \tag{21}$$

where $I_{\pm}$ is an nxn diagonal matrix whose diagonal components are either 1 or

- 1. Hence, Eq. 20 is a special case of Eq. 21 in which the diagonal members of $I_{\pm}$ are all equal to - 1. When Eq. 21 is valid, the stochastic field is referred to as a "quadrant field."[24] Assuming that an n-fold Fourier transform of $R_{f_0 f_0}(\underline{\xi})$ exists, the spectral density function of $f_0(\underline{x})$ is defined as:

$$S_{f_0 f_0}(\underline{\kappa}) = \frac{1}{(2\pi)^n} \int_{-\infty}^{\infty} R_{f_0 f_0}(\underline{\xi})\, e^{-i\underline{k}\cdot\underline{\xi}}\, d\underline{\xi} \tag{22}$$

and its inverse transform is given by:

$$R_{f_0 f_0}(\underline{\xi}) = \int_{-\infty}^{\infty} S_{f_0 f_0}(\underline{\kappa})\, e^{i\underline{\kappa}\cdot\underline{\xi}}\, d\underline{\kappa} \tag{23}$$

The preceding two equations represent the n-dimensional version of the Wiener-Khintchine transform pair, where $\underline{\kappa} = [\kappa_1 \quad \kappa_2 \quad \cdots \quad \kappa_n]^T$ is the wave number vector and $\underline{\kappa}\cdot\underline{\xi}$ is the inner product of $\underline{\kappa}$ and $\underline{\xi}$, and, for simplicity:

$$\int_{-\infty}^{\infty} (\,)d\underline{\xi} = \int_{-\infty}^{\infty} \overset{n\text{-fold}}{\cdots\cdots} \int_{-\infty}^{\infty} (\,)d\xi_1 d\xi_2 \cdots d\xi_n \tag{24}$$

$$\int_{-\infty}^{\infty} (\,)d\underline{\kappa} = \int_{-\infty}^{\infty} \overset{n\text{-fold}}{\cdots\cdots} \int_{-\infty}^{\infty} (\,)d\kappa_1 d\kappa_2 \cdots d\kappa_n \tag{25}$$

It can be easily shown that:

$$S_{f_0 f_0}(\underline{\kappa}) = S_{f_0 f_0}(-\underline{\kappa}) \tag{26}$$

and that the spectral density function is real. In addition, the following equation is obtained under the condition of Eq. 21:

$$S_{f_0 f_0}(\underline{\kappa}) = S_{f_0 f_0}(I_{\pm}\underline{\kappa}) \tag{27}$$

This equation indicates that the value of $S_{f_0 f_0}(\underline{\kappa})$ is identical at a corres-

ponding point in each quadrant ($\underline{\kappa} = I_{\pm}\,\underline{\kappa}$), hence the name "quadrant field."

Finally, it can be shown that the autocorrelation function $R_{f_0f_0}(\underline{\xi})$ is non-negative definite and has a non-negative n-dimensional Fourier transform, i.e.:

$$S_{f_0f_0}(\underline{\kappa}) \geq 0 \tag{28}$$

Based on these properties of $S_{f_0f_0}(\underline{\kappa})$, the n-dimensional homogeneous stochastic field $f_0(\underline{x})$ can be simulated by a stochastic field $f(\underline{x})$ in the following fashion: consider an nD-1V homogeneous field $f_0(\underline{x})$ with mean zero and spectral density function $S_{f_0f_0}(\underline{\kappa})$ which is of insignificant magnitude outside the region defined by:

$$-\underline{\kappa}_u \leq \underline{\kappa} \leq \underline{\kappa}_u \tag{29}$$

where $\underline{\kappa}_u = [\kappa_{1u}\ \kappa_{2u}\ \cdots\cdots\ \kappa_{nu}]^T$ with $\kappa_{iu} > 0$ $(i=1,2,\ldots,n)$. Denote the interval vector by:

$$(\Delta\kappa_1\ \ \Delta\kappa_2\ \ \cdots\ \ \Delta\kappa_n) = \left(\frac{\kappa_{1u}}{N_1}\ \ \frac{\kappa_{2u}}{N_2}\ \ \cdots\cdots\ \ \frac{\kappa_{nu}}{N_n}\right) \tag{30}$$

and then construct the simulated field $f(\underline{x})$ by the following series, as $N_1, N_2, \ldots, N_n \to \infty$ simultaneously:

$$f(\underline{x}) = \sqrt{2} \sum_{k_1=1}^{N_1} \sum_{k_2=1}^{N_2} \cdots\cdots \sum_{k_n=1}^{N_n} \sum_{\substack{I_1=1,\, I_i=\pm 1 \\ i=2,3,\ldots,n}} \left[2S_{f_0f_0}(I_1\kappa_{1k_1}, I_2\kappa_{2k_2}, \ldots\ldots, I_n\kappa_{nk_n})\Delta\kappa_1\Delta\kappa_2\cdots\Delta\kappa_n\right]^{1/2} \times$$

$$\times \cos\left(I_1\kappa_{1k_1}x_1 + I_2\kappa_{2k_2}x_2 + \cdots + I_n\kappa_{nk_n}x_n + \phi_{k_1k_2\cdots k_n}^{I_1I_2\cdots I_n}\right) \qquad (31)$$

where $\phi_{k_1k_2\cdots k_n}^{I_1I_2\cdots I_n}$ = independent random phase angles uniformly distributed between 0 and 2π, and

$$\kappa_{ik_i} = k_i\Delta\kappa_i, \qquad k_i = 1,2,\ldots,N_i, \qquad i = 1,2,\ldots,n. \qquad (32)$$

The simulated field $f(\underline{x})$ is asymptotically Gaussian as $N_1,N_2,\ldots,N_n \to \infty$ simultaneously again due to the central limit theorem. Note that a set of I_1, I_2, ..., I_n indicates one of the 2^n quadrants of the wave number $\underline{\kappa}$ space. Because $S(\underline{\kappa}) = S(-\underline{\kappa})$, we need to cover only 2^{n-1} quadrants, half of the total 2^n, for simulation purposes. Thus I_1 is always chosen to be unity ($I_1 = 1$). This also implies that (i) there are 2^{2n-1} sets of $N_1N_2\ldots N_n$ random phase angles in the expression for $f(\underline{x})$ given by Eq. 31 and (ii) twice the spectral density function always appears in the same equation.

If the stochastic field is quadrant, then $S_{f_0f_0}(I_1\kappa_{1k_1}, I_2\kappa_{2k_2}, \ldots, I_n\kappa_{nk_n})$ in Eq. 31 can be replaced by $S_{f_0f_0}(\kappa_{1k_1}, \kappa_{2k_2}, \ldots, \kappa_{nk_n})$. Also, if the stochastic field has a non-zero spectral density only over a pair of quadrants in the wave number domain for which $S_{f_0f_0}(\underline{\kappa}) = S_{f_0f_0}(-\underline{\kappa})$, then the stochastic field is referred to as "uni-quadrant" and Eq. 31 can be written as:

$$f(\underline{x}) = \sqrt{2}\sum_{k_1=1}^{N_1}\sum_{k_2=1}^{N_2}\cdots\sum_{k_n=1}^{N_n}\left[2S_{f_0f_0}(\kappa_{1k_1}, \kappa_{2k_2}, \ldots, \kappa_{nk_n})\Delta\kappa_1\Delta\kappa_2\cdots\Delta\kappa_n\right]^{\frac{1}{2}} \times$$

$$\times \cos\left(\kappa_{1k_1}x_1 + \kappa_{2k_2}x_2 + \cdots + \kappa_{nk_n}x_n + \phi_{k_1k_2\cdots k_n}\right) \qquad (33)$$

For example, a 2D-1V stochastic field is uni-quadrant if the spectral density is non-zero only over the first quadrant (and therefore over the third quadrant).

Referring to 2D-1V homogeneous stochastic fields, Eq. 31 can be written explicitly as

$$f(\underline{x}) = \sqrt{2} \sum_{k_1=1}^{N_1} \sum_{k_2=1}^{N_2} \{[2S_{f_0f_0}(\kappa_{1k_1},\kappa_{2k_2})\Delta\kappa_1\Delta\kappa_2]^{\frac{1}{2}} \times$$

$$\times \cos(\kappa_{1k_1}x_1 + \kappa_{2k_2}x_2 + \phi^{(1)}_{k_1k_2}) + [2S_{f_0f_0}(\kappa_{1k_1},-\kappa_{2k_2})\Delta\kappa_1\Delta\kappa_2]^{\frac{1}{2}} \times$$

$$\times \cos(\kappa_{1k_1}x_1 - \kappa_{2k_2}x_2 + \phi^{(2)}_{k_1k_2})\} \tag{34}$$

Furthermore, if the stochastic field is quadrant,

$$f(\underline{x}) = \sqrt{2} \sum_{k_1=1}^{N_1} \sum_{k_2=1}^{N_2} [2S_{f_0f_0}(\kappa_{1k_1},\kappa_{2k_2})\Delta\kappa_1\Delta\kappa_2]^{\frac{1}{2}} \times$$

$$\times \{\cos(\kappa_{1k_1}x_1 + \kappa_{2k_2}x_2 + \phi^{(1)}_{k_1k_2}) + \cos(k_{1k_1}x_1 - \kappa_{2k_2}x_2 + \phi^{(2)}_{k_1k_2})\} \tag{35}$$

where $\phi^{(1)}_{k_1k_2} = \phi^{1,1}_{k_1k_2}$ and $\phi^{(2)}_{k_1k_2} = \phi^{1,-1}_{k_1k_2}$ if the notation introduced in Eq. 31 is to be used. Finally, if the field is uni-quadrant over the first quadrant:

$$f(\underline{x}) = \sqrt{2} \sum_{k_1=1}^{N_1} \sum_{k_2=1}^{N_2} [2S_{f_0f_0}(\kappa_{1k_1},\kappa_{2k_2})\Delta\kappa_1\Delta\kappa_2]^{\frac{1}{2}} \times$$

$$\times \cos(\kappa_{1k_1}x_1 + \kappa_{2k_2}x_2 + \phi_{k_1k_2}) \tag{36}$$

In a way similar to the one used for the 1D-1V processes, it can be shown that the expected value and autocorrelation function of the simulated field are the same with the target ones, i.e., $E[f(\underline{x})] = E[f_0(\underline{x})] = 0$ and $R_{ff}(\underline{\xi}) = R_{f_0f_0}(\underline{\xi})$. Also, the nD-1V simulated field is ergodic[14], at least to the second moment, and the computational cost for the digital generation of sample functions of

the stochastic field $f(\underline{x})$ can be dramatically reduced by applying the FFT technique to the appropriate trigonometric series expression[13].

2.3 Simulation of nD-mV Homogeneous Stochastic Fields Using Spectral Representation

The simulation of nD-mV (n-dimensional and m-variate) homogeneous stochastic fields[14], unlike the case of nD-1V fields, cannot be achieved by straightforward generalization of the 1D-1V case, as shown below.

Consider a set of m homogeneous Gaussian n-dimensional stochastic fields $f_j^0(\underline{x})$ $(j=1,2,\ldots,m)$ with mean zero:

$$E[f_j^0(\underline{x})] = 0 \tag{37}$$

and with cross-spectral density matrix $\underline{S}^0(\underline{\kappa})$ defined by:

$$\underline{S}^0(\underline{\kappa}) = \begin{bmatrix} S_{11}^0(\underline{\kappa}) & S_{12}^0(\underline{\kappa}) & \cdots\cdots\cdots & S_{1m}^0(\underline{\kappa}) \\ S_{21}^0(\underline{\kappa}) & S_{22}^0(\underline{\kappa}) & \cdots\cdots\cdots & S_{2m}^0(\underline{\kappa}) \\ \cdots\cdots & \cdots\cdots & \cdots\cdots & \cdots\cdots \\ S_{m1}^0(\underline{\kappa}) & S_{m2}^0(\underline{\kappa}) & \cdots\cdots\cdots & S_{mm}^0(\underline{\kappa}) \end{bmatrix} \tag{38}$$

where $S_{jk}^0(\underline{\kappa})$ is the n-dimensional Wiener-Khintchine transform of the cross-correlation function $R_{jk}^0(\underline{\xi})$ $(j\neq k)$ or the auto-correlation function $R_{jk}^0(\underline{\xi})$ $(j=k)$.

Due to the assumption of homogeneity:

$$R_{jk}^0(\underline{\xi}) = R_{kj}^0(-\underline{\xi}), \tag{39}$$

the following expression can be obtained:

$$S_{jk}^0(\underline{\kappa}) = \bar{S}_{kj}^0(\underline{\kappa}) \tag{40}$$

where the super bar indicates the complex conjugate. The matrix $\underline{S}^0(\underline{\kappa})$ is

therefore Hermitian. It can be shown that $\underline{S}^0(\underline{\kappa})$ is also non-negative definite.

Suppose now one can find a matrix $\underline{H}(\underline{\kappa})$ which possesses an n-dimensional Fourier transform and satisfies the equation:

$$\underline{S}^0(\underline{\kappa}) = \underline{H}(\underline{\kappa})\overline{\underline{H}}(\underline{\kappa})^T \tag{41}$$

where $\underline{S}^0(\underline{\kappa})$ is the specified target cross-spectral density matrix and T indicates the transpose. Then, $f_j^0(\underline{x})$ (j=1,2,...,m) can be simulated by $f_j(\underline{x})$ given below.

$$f_j(\underline{x}) = \sum_{k=1}^{m} \int_{-\infty}^{x} h_{jk}(\underline{x}-\underline{\xi})\eta_k(\underline{\xi})d\underline{\xi} \tag{42}$$

where $h_{jk}(\underline{x})$ is the n-dimensional Fourier transform of $H_{jk}(\underline{\kappa})$:

$$h_{jk}(\underline{x}) = \int_{-\infty}^{\infty} H_{jk}(\underline{\kappa})e^{-i\underline{\kappa}\cdot\underline{x}}\, d\underline{\kappa} \tag{43}$$

In Eq. 42, $\eta_k(\underline{x})$ are independent n-dimensional Gaussian white noises such that:

$$E[\eta_j(\underline{x}_1)\eta_k(\underline{x}_2)] = \delta(\underline{x}_1 - \underline{x}_2)\delta_{jk} \tag{44}$$

with:

$$\delta(\underline{x}_1-\underline{x}_2) = \delta(x_{11}-x_{21})\delta(x_{12}-x_{22}) \cdots \delta(x_{1n}-x_{2n}) \tag{45}$$

where $\delta(\cdot)$ and δ_{ij} are the delta function and Kronecker's delta, respectively. Since $\eta_k(\underline{x})$ are Gaussian, $f_j(\underline{x})$ are also Gaussian. It can be easily verified that $f_j(\underline{x})$ (j=1,2,...,m), as simulated by Eq. 42, satisfies Eqs. 37 and 41 and thus simulates $f_j^0(\underline{x})$ up to the second moments. Hence, if $f_j^0(\underline{x})$ is Gaussian, $f_j(\underline{x})$ is identical with $f_j^0(\underline{x})$.

To find the matrix $\underline{H}(\underline{\kappa})$ in an efficient way, we assume that $H(\underline{\kappa})$ is a

lower triangular matrix:

$$\underline{H}(\underline{\kappa}) = \begin{bmatrix} H_{11}(\underline{\kappa}) & 0 & 0 & \cdots & 0 \\ H_{21}(\underline{\kappa}) & H_{22}(\underline{\kappa}) & \cdots & \cdots & 0 \\ \cdots & \cdots & \cdots & \cdots & \cdots \\ H_{m1}(\underline{\kappa}) & H_{m2}(\underline{\kappa}) & \cdots & \cdots & H_{mm}(\underline{\kappa}) \end{bmatrix} \tag{46}$$

By substituting the above into Eq. 41, solutions are obtained[10] as:

$$H_{kk}(\underline{\kappa}) = \left[\frac{D_k(\underline{\kappa})}{D_{k-1}(\underline{\kappa})}\right]^{1/2} \qquad k=1,2,\ldots,m \tag{47}$$

where $D_k(\underline{\kappa})$ is the k-th principal minor of $\underline{S}^0(\underline{\kappa})$ with D_0 being defined as unity, and

$$H_{jk}(\underline{\kappa}) = H_{kk}(\underline{\kappa}) \frac{S^0\begin{pmatrix}1,2,\ldots,k-1,j\\1,2,\ldots,k-1,k\end{pmatrix}}{D_k(\underline{\kappa})} \qquad \begin{matrix}k=1,2,\ldots,m\\ j=k+1,\ldots,m\end{matrix} \tag{48}$$

where

$$S^0\begin{pmatrix}1,2,\ldots,k-1,j\\1,2,\ldots,k-1,k\end{pmatrix} = \begin{vmatrix} S^0_{11} & S^0_{12} & \cdots & S^0_{1,k-1} & S^0_{1k} \\ S^0_{21} & S^0_{22} & \cdots & S^0_{2,k-1} & S^0_{2k} \\ \cdots & \cdots & \cdots & \cdots & \cdots \\ S^0_{k-1,1} & S^0_{k-1,2} & \cdots & S^0_{k-1,k-1} & S^0_{k-1,k} \\ S^0_{j1} & S^0_{j2} & \cdots & S^0_{j,k-1} & S^0_{jk} \end{vmatrix} \tag{49}$$

is the determinant of a submatrix obtained by deleting all the elements except the $(1,2,\ldots,k-1,j)$-th row and $(1,2,\ldots,k-1,k)$-th column of $\underline{S}^0(\underline{\kappa})$. It is noted that the above decomposition is valid only when the matrix $\underline{S}^0(\underline{\kappa})$ is Hermitian and positive definite as can be seen from Eq. 47.

Because the cross-spectral density matrix $\underline{S}^0(\underline{\kappa})$ is known to be only non-

negative definite, special consideration is needed in those cases where $\underline{S}^0(\underline{\kappa})$ has a zero principal minor[14].

Once $\underline{H}(\underline{\kappa})$ is computed using Eqs. 47 and 48, instead of passing a white noise vector through filters, the field $f_j(\underline{x})$ can be simulated in a more efficient way by the following series, as $N_1, N_2, \ldots, N_n \to \infty$ simultaneously and under the assumption that the stochastic field possesses quadrant symmetry:

$$f_j(\underline{x}) = 2 \sum_{m=1}^{j} \sum_{\ell_1=1}^{N_1} \sum_{\ell_2=1}^{N_2} \cdots \sum_{\ell_n=1}^{N_n} \sum_{\substack{I_1=1, I_i=\pm 1 \\ i=2,3,\ldots,n}} \left| H_{jm}(\kappa_{1\ell_1}, \kappa_{2\ell_2}, \ldots, \kappa_{n\ell_n}) \right| \cdot$$

$$\cdot \sqrt{\Delta\kappa_1 \Delta\kappa_2 \cdots \Delta\kappa_n} \cdot \cos\left[I_1 \kappa_{1\ell_1} x_1 + I_2 \kappa_{2\ell_2} x_2 + \cdots + I_n \kappa_{n\ell_n} x_n + \right.$$

$$\left. + \theta_{jm}(\kappa_{1\ell_1}, \kappa_{2\ell_2}, \ldots, \kappa_{n\ell_n}) + \phi_{m\ell_1\ell_2\ldots\ell_n}^{I_1 I_2 \ldots I_n} \right] \tag{50}$$

where:

$$(\Delta\kappa_1 \quad \Delta\kappa_2 \quad \cdots \quad \Delta\kappa_n) = \left(\frac{\kappa_{1u}}{N_1} \quad \frac{\kappa_{2u}}{N_2} \quad \cdots \quad \frac{\kappa_{nu}}{N_n}\right) \tag{51}$$

$$\kappa_{i\ell_i} = \ell_i \Delta\kappa_i \; ; \qquad \ell = 1, 2, \ldots, N_i \; ; \qquad i = 1, 2, \ldots, n \tag{52}$$

$$\theta_{jm}(\kappa_{1\ell_1}, \kappa_{2\ell_2}, \ldots, \kappa_{n\ell_n}) = \tan^{-1}\left[\frac{\text{Im } H_{jm}(\kappa_{1\ell_1}, \kappa_{2\ell_2}, \ldots, \kappa_{n\ell_n})}{\text{Re } H_{jm}(\kappa_{1\ell_1}, \kappa_{2\ell_2}, \ldots, \kappa_{n\ell_n})} \right] \tag{53}$$

$\phi_{m\ell_1\ell_2\ldots\ell_n}^{I_1 I_2 \ldots I_n}$ = independent random phase angles uniformly distributed between 0 and 2π. The simulated field $f_j(\underline{x})$ is asymptotically Gaussian as $N_1, N_2, \ldots, N_n \to \infty$ simultaneously, again due to the central limit theorem.

Finally, it can be shown again that the expected value and autocorrelation function of the simulated field (using Eq. 50) are the same as the target ones, i.e., $E[f_j(\underline{x})] = E[f_j^0(\underline{x})] = 0$ and $R_{jk}(\underline{\xi}) = R_{jk}^0(\underline{\xi})$; $j,k = 1, 2, \ldots, m$. Al-

so, it can be shown that the simulated field is ergodic[14] at least to the second moment. Here again, the computational effort for the digital generation of sample functions of the stochastic field $f_j(\underline{x})$ can be substantially reduced by applying the FFT technique to Eq. 50.

3. SIMULATION OF SEISMIC GROUND MOTION USING NON-STATIONARY PROCESS AND NON-HOMOGENEOUS FIELD MODELS

3.1 Simulation of 1D-1V Nonstationary Stochastic Processes Using Spectral Representation

A more realistic simulation of seismic ground motion can be made by considering nonstationary stochastic processes or nonhomogeneous stochastic fields. From the engineering point of view, it is highly desirable that such non-stationary and non-homogeneous models permit physical interpretation of their spectral contents as closely as possible to, or as a straightforward extension of, the power spectra associated with stationary stochastic processes or homogeneous stochastic fields. Among the various attempts to define such non-stationary and non-homogeneous spectra, it is the "evolutionary spectrum" developed by Priestley[25,26] that appears to offer the most palatable transition from the power spectra associated with stationary and homogeneous stochastic processes and fields to those associated with non-stationary and non-homogeneous stochastic processes and fields. This is the reason why evolutionary power will be used exclusively in the following.

A brief description of a 1D-1V nonstationary stochastic process $y_0(t)$ with evolutionary power is given below to introduce certain notions appearing in the theory of evolutionary power.

If a stochastic process (stationary or non-stationary) can be represented as:

$$y_0(t) = \int_{-\infty}^{\infty} A(t,\omega)e^{i\omega t}\, dZ(\omega) \tag{54}$$

where $A(t,\omega)$ is a modulating function and $dZ(\omega)$ represents an orthogonal increment, the process $y_0(t)$ is said to be oscillatory. Note that the physical

notion of frequency has been preserved by including the complex exponential, and that if $A(t,\omega)$ is constant, $y_0(t)$ is a stationary process. The mean square of the oscillatory process is found to be:

$$E[y_0^2(t)] = \int_{-\infty}^{\infty} |A(t,\omega)|^2 \, dF(\omega) \tag{55}$$

where $dF(\omega) = E[dZ(\omega)]^2$. By introducing the evolutionary spectrum in the form:

$$dF^0(t,\omega) = |A(t,\omega)|^2 \, dF(\omega) \tag{56}$$

the non-stationary spectral contents are defined. Equation 56 may be written as:

$$f^0(t,\omega)d\omega = |A(t,\omega)|^2 f(\omega)d\omega \tag{57}$$

if $f(\omega)$ exists such that $dF(\omega) = f(\omega)d\omega$, where $dF^0(t,\omega) = f^0(t,\omega)d\omega$. In this case, it can also be shown that an oscillatory process $y_0(t)$ of the form of Eq. 54 has the following auto-correlation function.

$$R_{y_0y_0}(t+\tau,t) = \int_{-\infty}^{\infty} A(t+\tau,\omega)A(t,\omega)e^{i\omega\tau} \, f(\omega)d\omega \tag{58}$$

It is of major importance to recognize that if the evolutionary power spectrum can be expressed in the form of Eq. 57, then the autocorrelation function $R_{y_0y_0}(t+\tau,t)$ can be calculated using Eq. 58. This is significant since it is usually the evolutionary power spectrum of an earthquake that can be estimated or measured and not its autocorrelation function[27].

As far as the simulation procedure is concerned, the method that has been proposed in Section 2.1 for 1D-1V stationary processes can be directly gen-

eralized to a non-stationary process characterized by an evolutionary power spectrum[10]. Thus, if a non-stationary process $y_0(t)$ has an evolutionary power spectrum of the form shown in Eq. 57, then the process can be simulated by the following expression, as $N \to \infty$.

$$y(t) = \sqrt{2} \sum_{j=1}^{N} \sqrt{2A^2(t,\omega_j)f(\omega_j)\Delta\omega}\cos(\omega_j t + \phi_j) \tag{59}$$

where $\omega_j = j\Delta\omega$; $j=1,2,\ldots,N$. An upper bound of the frequency $\omega_u = N\cdot\Delta\omega$ is again implicit in Eq. 59 and ϕ_j are independent random phase angles uniformly distributed over the range $(0,2\pi)$. Note that the simulated process $y(t)$ is asymptotically Gaussian as N becomes large due to the central limit theorem. It can be shown that the simulated process $y(t)$ possesses the target evolutionary power spectrum as $N \to \infty$.

3.2 Simulation of nD-1V Nonhomogeneous Stochastic Fields Using Spectral Representation

The evolutionary power spectrum theory for 1D-1V nonstationary stochastic processes, presented in the preceding section, will now be extended to nD-1V nonhomogeneous stochastic fields below. If an nD-1V nonhomogeneous stochastic field can be represented in the form:

$$y_0(\underline{x}) = \int_{-\infty}^{\infty} A(\underline{x},\underline{\kappa})e^{i\underline{\kappa}\cdot\underline{x}}\, dZ(\underline{\kappa}) \tag{60}$$

where $A(\underline{x},\underline{\kappa})$ is a modulating function and $dZ(\underline{\kappa})$ represents an orthogonal increment, then the stochastic field $y_0(\underline{x})$ is called oscillatory. The mean square of the oscillatory field is given by:

$$E[y_0^2(\underline{x})] = \int_{-\infty}^{\infty} \left|A(\underline{x},\underline{\kappa}\right|^2 \, dF(\underline{\kappa}) \tag{61}$$

where

$$dF(\underline{\kappa}) = E[dZ(\underline{\kappa})]^2 \tag{62}$$

By introducing the evolutionary power spectrum of the nD-1V nonhomogeneous stochastic field in the form:

$$dF^0(\underline{x},\underline{\kappa}) = \left|A(\underline{x},\underline{\kappa})\right|^2 \, dF(\underline{\kappa}) \tag{63}$$

the nonhomogeneous spectral contents are defined. Equation 63 can be written as:

$$f^0(\underline{x},\underline{\kappa})d\underline{\kappa} = \left|A(\underline{x},\underline{\kappa})\right|^2 \, f(\underline{\kappa})d\underline{\kappa} \tag{64}$$

if $f(\underline{\kappa})$ exists such that $dF(\underline{\kappa}) = f(\underline{\kappa})d\underline{\kappa}$, where $dF^0(\underline{x},\underline{\kappa}) = F^0(\underline{x},\underline{\kappa})d\underline{\kappa}$. Under these conditions, it can be shown that an oscillatory stochastic field $y_0(\underline{x})$ has the following autocorrelation function,

$$R_{y_0y_0}(\underline{x}+\underline{\xi},\underline{x}) = \int_{-\infty}^{\infty} A(\underline{x}+\underline{\xi},\underline{\kappa})A(\underline{x},\underline{\kappa})e^{i\underline{\kappa}\cdot\underline{\xi}} \, f(\underline{\kappa})d\underline{\kappa} \tag{65}$$

The stochastic field $y_0(\underline{x})$ can be simulated in the following way, as $N_1, N_2, \ldots, N_n \to \infty$ simultaneously and under the assumption that the stochastic field is quadrant symmetric:

$$y(\underline{x}) = \sqrt{2} \sum_{\ell_1=1}^{N_1} \sum_{\ell_2=1}^{N_2} \cdots \sum_{\ell_n=1}^{N_n} \sum_{\substack{I_1=1, I_i=\pm 1 \\ i=2,3,\ldots,n}} \sqrt{2A^2(x_1,x_2,\ldots,x_n,\kappa_{1\ell_1},\kappa_{2\ell_2},\ldots,\kappa_{n\ell_n})}$$

$$\cdot \sqrt{f(\kappa_{1\ell_1},\kappa_{2\ell_2},\ldots,\kappa_{n\ell_n})\Delta\kappa_1\Delta\kappa_2\cdots\Delta\kappa_n} \cdot \cos[I_1\kappa_{1\ell_1}x_1 + I_2\kappa_{2\ell_2}x_2 + \cdots$$

$$\cdots + I_n \kappa_{n\ell_n} x_n + \phi^{I_1 I_2 \cdots I_n}_{\ell_1 \ell_2 \cdots \ell_n}] \tag{66}$$

where:

$$(\Delta\kappa_1 \ \Delta\kappa_2 \ \cdots \ \Delta\kappa_n) = \left(\frac{\kappa_{1u}}{N_1} \ \frac{\kappa_{2u}}{N_2} \ \cdots \ \frac{\kappa_{nu}}{N_n}\right) \tag{67}$$

$$\kappa_{i\ell_i} = \ell_i \Delta\kappa_i \ ; \qquad \ell_i = 1,2,\ldots,N_i; \quad i=1,2,\ldots,n \tag{68}$$

$\phi^{I_1 I_2 \cdots I_n}_{\ell_1 \ell_2 \cdots \ell_n}$ = independent random phase angles uniformly distributed in the range $(0,2\pi)$.

Referring to 2D-1V nonhomogeneous stochastic fields, Eq. 66 can be written as (quadrant symmetry is assumed):

$$y(x_1,x_2) = \sqrt{2} \sum_{\ell_1=1}^{N_1} \sum_{\ell_2=2}^{N_2} \sqrt{2A^2(x_1,x_2,\kappa_{1\ell_1},\kappa_{2\ell_2}) \cdot f(\kappa_{1\ell_1},\kappa_{2\ell_2})\Delta\kappa_1\Delta\kappa_2} \cdot$$

$$\cdot \{\cos[\kappa_{1\ell_1} x_1 + \kappa_{2\ell_2} x_2 + \phi^{(1)}_{\ell_1\ell_2}] + \cos[\kappa_{1\ell_1} x_1 - \kappa_{2\ell_2} x_2 + \phi^{(2)}_{\ell_1\ell_2}]\} \tag{69}$$

where $\phi^{(1)}_{\ell_1\ell_2} = \phi^{1,1}_{\ell_1\ell_2}$ and $\phi^{(2)}_{\ell_1\ell_2} = \phi^{1,-1}_{\ell_1\ell_2}$ if the notation introduced in Eq. 66 is to be used. Note again that the simulated field $y(\underline{x})$ is asymptotically Gaussian as $N_1,N_2,\ldots,N_n \to \infty$ simultaneously, due to the central limit theorem. Finally, it can be shown that the simulated field $y(\underline{x})$ possesses the target evolutionary power spectrum as $N_1,N_2,\ldots,N_n \to \infty$ simultaneously.

4. SIMULATION OF SEISMIC GROUND MOTION USING STOCHASTIC WAVES

4.1 Theory of nD-1V Stochastic Waves

An even more realistic simulation of seismic ground motion can be obtained by explicitly describing it as a stochastic propagating wave. For this purpose, consider the following spatially n-dimensional stochastic wave:

$$y_0(\underline{x}^*) = \int_{-\infty}^{\infty} A(\underline{x}^*, \underline{\kappa}^*) e^{i\underline{\kappa}^* \cdot \underline{x}^*} \, dZ(\underline{\kappa}^*) \tag{70}$$

where $\underline{x}^* = [t, x_1, x_2, \ldots, x_n]^T$ is an (n+1)-dimensional vector containing the time variable (t) and n space variables (x's) and $\underline{\kappa}^* = [\omega, \kappa_1, \kappa_2, \ldots, \kappa_n]^T$ is an (n+1)-dimensional vector containing the frequency (ω) and n wave numbers (κ's). The frequency corresponds to the time variable, while the n wave numbers correspond to the n space variables.

Note again that Eq. 70 is a direct generalization of Eq. 54 into the multi-dimensional case. Therefore, $A(\underline{x}^*, \underline{\kappa}^*)$ is a modulating function, $dZ(\underline{\kappa}^*)$ represents an orthogonal increment and $y_0(\underline{x}^*)$ is an "oscillatory" stochastic wave in the sense of Priestley's definition.

The mean square of the oscillatory stochastic wave is:

$$E[y_0^2(\underline{x}^*)] = \int_{-\infty}^{\infty} \left| A(\underline{x}^*, \underline{\kappa}^*) \right|^2 \, dF(\underline{\kappa}^*) \tag{71}$$

where:

$$dF(\underline{\kappa}^*) = E[dZ(\underline{\kappa}^*)]^2 \tag{72}$$

Now, by introducing the (n+1)-dimensional evolutionary power spectrum in the form:

$$dF^0(\underline{x}^*,\underline{\kappa}^*) = \left|A(\underline{x}^*,\underline{\kappa}^*)\right|^2 dF(\underline{\kappa}^*) \tag{73}$$

the nonstationary and/or nonhomogeneous spectral contents are defined. Equation 73 can be written as:

$$dF^0(\underline{x}^*,\underline{\kappa}^*) = f^0(\underline{x}^*,\underline{\kappa}^*)d\underline{\kappa}^* = \left|A(\underline{x}^*,\underline{\kappa}^*)\right|^2 f(\underline{\kappa}^*)d\underline{\kappa}^* \tag{74}$$

if $f(\underline{\kappa}^*)$ exists such that:

$$dF(\underline{\kappa}^*) = f(\underline{\kappa}^*)d\underline{\kappa}^* \tag{75}$$

It can also be shown that an oscillatory stochastic wave $y_0(\underline{x}^*)$ of the form appearing in Eq. 70 has the following autocorrelation function, if Eq. 75 is valid:

$$R_{y_0y_0}(\underline{x}^*+\underline{\xi}^*,\underline{x}^*) = \int_{-\infty}^{\infty} A(\underline{x}^*+\underline{\xi}^*,\underline{\kappa}^*)A(\underline{x}^*,\underline{\kappa}^*) \cdot e^{i\underline{\xi}^*\cdot\underline{\kappa}^*} \cdot f(\underline{\kappa}^*)d\underline{\kappa}^* \tag{76}$$

where the separation vector $\underline{\xi}^*$ is given by:

$$\underline{\xi}^* = \left[\tau\ \xi_1\ \xi_2\ \cdots\ \xi_n\right]^T \tag{77}$$

At this juncture, it should be pointed out that if the stochastic wave is stationary in terms of time and/or homogeneous in terms of certain space variables, then the modulating function $A(\underline{x}^*,\underline{\kappa}^*)$ has to be independent of the time variable and/or these space variables, and also independent of the corresponding elements of the $\underline{\kappa}^*$ vector.

The stochastic wave $y_0(\underline{x}^*)$ can be simulated in the following way as N_t, $N_1,N_2,\ldots,N_n \to \infty$ simultaneously and under the assumption that the stochastic wave is quadrant symmetric in terms of the space variables:

$$y(\underline{x}^*) = \sqrt{2} \sum_{m=1}^{N_t} \sum_{\ell_1=1}^{N_1} \sum_{\ell_2=1}^{N_2} \cdots \sum_{\ell_n=1}^{N_n} \sum_{\substack{I_1=1, I_i=\pm 1 \\ i=2,3,\ldots,n}}$$

$$\sqrt{2A^2(t, x_1, x_2, \ldots, x_n, \omega_m, \kappa_{1\ell_1}, \kappa_{2\ell_2}, \ldots, \kappa_{n\ell_n})} \cdot$$

$$\cdot \sqrt{f(\omega_m, \kappa_{1\ell_1}, \kappa_{2\ell_2}, \ldots, \kappa_{n\ell_n}) \Delta\omega \Delta\kappa_1 \Delta\kappa_2 \cdots \Delta\kappa_n} \cdot$$

$$\cdot \cos\left[\omega_m t + I_1 \kappa_{1\ell_1} x_1 + I_2 \kappa_{2\ell_2} x_2 + \cdots + I_n \kappa_{n\ell_n} x_n + \phi^{I_1 I_2 \cdots I_n}_{m\ell_1 \ell_2 \cdots \ell_n}\right] \tag{78}$$

where:

$$(\Delta\omega \ \Delta\kappa_1 \ \Delta\kappa_2 \cdots \Delta\kappa_n) = \left(\frac{\omega_u}{N_t} \ \frac{\kappa_{1u}}{N_1} \ \frac{\kappa_{2u}}{N_2} \ \cdots \ \frac{\kappa_{nu}}{N_n}\right) \tag{79}$$

$$\omega_m = m\Delta\omega \ ; \qquad m=1,2,\ldots,N_t \tag{80}$$

$$\kappa_{i\ell_i} = \ell_i \Delta\kappa_i \ ; \qquad \ell_i = 1,2,\ldots,N_i \ ; \qquad i=1,2,\ldots,n \tag{81}$$

$\phi^{I_1 I_2 \cdots I_n}_{m\ell_1 \ell_2 \cdots \ell_n}$ = independent random phase angles uniformly distributed in the range $(0, 2\pi)$

The simulated stochastic wave $y(\underline{x}^*)$ is asymptotically Gaussian as $N_t, N_1, \ldots, N_n \to \infty$ simultaneously, due to the central limit theorem. It is shown below that the autocorrelation function of the simulated stochastic wave is the same with the target autocorrelation function $R_{y_0 y_0}(\underline{x}^* + \underline{\xi}^*, \underline{x}^*)$ given by Eq. 76. For this purpose, Eq. 78 is written in condensed form as (assuming uniquadrant symmetry for simplicity):

$$y(\underline{x}^*) = \sqrt{2} \sum_{\ell=1}^{N} \sqrt{2A^2(\underline{x}^*, \underline{\kappa}^*_\ell) f(\underline{\kappa}^*_\ell) \Delta\kappa^*} \cdot \cos\left[\underline{\kappa}^*_\ell \cdot \underline{x}^* + \phi_\ell\right] \tag{82}$$

where $N = N_t N_1 N_2 \ldots N_n$. The autocorrelation function of the simulated stochastic wave is:

$$R_{yy}(\underline{x}^*+\underline{\xi}^*,\underline{x}^*) = E\left[y(\underline{x}^*)y(\underline{x}^*+\underline{\xi}^*)\right] =$$

$$= E\left\{\sqrt{2}\sum_{\ell=1}^{N}\sqrt{2A^2(\underline{x}^*,\underline{\kappa}_\ell^*)f(\underline{\kappa}_\ell^*)\Delta\underline{\kappa}^*}\cdot\cos\left[\underline{\kappa}_\ell^*\cdot\underline{x}^* + \phi_\ell\right]\cdot\right.$$

$$\left.\cdot\sqrt{2}\sum_{m=1}^{N}\sqrt{2A^2(\underline{x}^*+\underline{\xi}^*,\underline{\kappa}_m^*)f(\underline{\kappa}_m^*)\Delta\underline{\kappa}^*}\cdot\cos\left[\underline{\kappa}_m^*\cdot(\underline{x}^*+\underline{\xi}^*) + \phi_m\right]\right\} =$$

$$= 2\sum_{\ell=1}^{N}\sum_{m=1}^{N}\sqrt{2^2\cdot A^2(\underline{x}^*,\underline{\kappa}_\ell^*)\cdot A^2(\underline{x}^*+\underline{\xi}^*,\underline{\kappa}_m^*)\cdot f(\underline{\kappa}_\ell^*)\cdot f(\underline{\kappa}_m^*)}\cdot\Delta\underline{\kappa}^*$$

$$\cdot E\left\{\cos\left[\underline{\kappa}_\ell^*\cdot\underline{x}^* + \phi_\ell\right]\cdot\cos\left[\underline{\kappa}_m^*\cdot(\underline{x}^*+\underline{\xi}^*) + \phi_m\right]\right\} \tag{83}$$

The expectation appearing in Eq. 83 can be written as follows:

$$\frac{1}{2}E\left\{\cos\left[\underline{\kappa}_\ell^*\cdot\underline{x}^*+\underline{\kappa}_m^*\cdot(\underline{x}^*+\underline{\xi}^*) + \phi_\ell + \phi_m\right] + \right.$$
$$\left. + \cos\left[\underline{\kappa}_\ell^*\cdot\underline{x}^*-\underline{\kappa}_m^*\cdot(\underline{x}^*+\underline{\xi}^*) + \phi_\ell - \phi_m\right]\right\} \tag{84}$$

It is easy to show that the expected value shown in Eq. 84 is different from zero only for $\ell=m$, for which it takes the following value:

$$\frac{1}{2}\cdot\cos\left[\underline{\kappa}_\ell^*\cdot\underline{x}^* - \underline{\kappa}_\ell^*\cdot(\underline{x}^*+\underline{\xi}^*)\right] = \frac{1}{2}\cdot\cos\left[\underline{\kappa}_\ell^*\cdot\underline{\xi}^*\right] \tag{85}$$

Substituting Eq. 85 into Eq. 83, the following expression is obtained for $R_{yy}(\underline{x}^*+\underline{\xi}^*,\underline{x}^*)$:

$$R_{yy}(\underline{x}^*+\underline{\xi}^*,\underline{x}^*) = \sum_{\ell=1}^{N} 2A(\underline{x}^*,\underline{\kappa}_\ell^*)\cdot A(\underline{x}^*+\underline{\xi}^*,\underline{\kappa}_\ell^*)\cdot f(\underline{\kappa}_\ell^*)\cdot\Delta\underline{\kappa}^*\cdot\cos\left[\underline{\kappa}_\ell^*\cdot\underline{\xi}^*\right] \tag{86}$$

In the limit as $N \to \infty$ and with the values of $\underline{\kappa}_u^*$ fixed, the preceding equation becomes:

$$R_{yy}(\underline{x}^*+\underline{\xi}^*,\underline{x}^*) = 2\int_0^\infty A(\underline{x}^*,\underline{\kappa}^*) \cdot A(\underline{x}^*+\underline{\xi}^*,\underline{\kappa}^*) \cdot f(\underline{\kappa}^*) \cdot \cos(\underline{\kappa}^*\cdot\underline{\xi}^*)d\underline{\kappa}^* \quad (87)$$

Under the assumption that the integrand in Eq. 87 is an even function of $\underline{\kappa}^*$, Eq. 87 yields:

$$R_{yy}(\underline{x}^*+\underline{\xi}^*,\underline{x}^*) = \int_{-\infty}^{\infty} A(\underline{x}^*,\underline{\kappa}^*) \cdot A(\underline{x}^*+\underline{\xi}^*,\underline{\kappa}^*) \cdot e^{i\underline{\kappa}^*\cdot\underline{\xi}^*} \cdot f(\underline{\kappa}^*)d\underline{\kappa}^* =$$

$$= R_{y_0y_0}(\underline{x}^*+\underline{\xi}^*,\underline{x}^*) \quad (88)$$

4.2 Application to Spatially One-Dimensional Stochastic Waves

Having presented above the general multi-dimensional theory of stochastic waves, a specific example is examined now, considering a spatially one-dimensional stochastic wave. In this case, $\underline{x}^*$ contains the time variable t and the space variable x, i.e.:

$$\underline{x}^* = [t \quad x]^T \quad (89)$$

and therefore the $\underline{\kappa}^*$ vector is given by:

$$\underline{\kappa}^* = [\omega \quad \kappa]^T \quad (90)$$

Then, the evolutionary power spectrum of $y_0(t,x)$ can be written as:

$$f(t,x,\omega,\kappa)d\omega d\kappa = \left|A(t,x,\omega,\kappa)\right|^2 f(\omega,\kappa)d\omega d\kappa \quad (91)$$

and the corresponding autocorrelation function as:

$$R_{y_0y_0}(t,t+\tau,x,x+\xi) = \int_{-\infty}^{\infty}\int_{-\infty}^{\infty} A(t+\tau,x+\xi,\omega,\kappa) \cdot A(t,x,\omega,\kappa) \cdot$$

$$\cdot e^{i[\omega\tau+\kappa\xi]} \cdot f(\omega,\kappa)d\omega d\kappa \quad (92)$$

If the stochastic wave is stationary and non-homogeneous, its evolutionary power spectrum becomes:

$$f(x,\omega,\kappa)d\omega d\kappa = \left|A(x,\kappa)\right|^2 f(\omega,\kappa)d\omega d\kappa \tag{93}$$

and the corresponding autocorrelation function takes the form:

$$R_{y_0y_0}(\tau,x,x+\xi) = \int_{-\infty}^{\infty}\int_{-\infty}^{\infty} A(x+\xi,\kappa) \cdot A(x,\kappa) \cdot e^{i[\omega\tau+\kappa\xi]} \cdot f(\omega,\kappa)d\omega d\kappa \tag{94}$$

If the stochastic wave is homogeneous and non-stationary, its evolutionary power spectrum becomes:

$$f(t,\omega,\kappa)d\omega d\kappa = \left|A(t,\omega)\right|^2 \cdot f(\omega,\kappa)d\omega d\kappa \tag{95}$$

and the corresponding autocorrelation function takes the form:

$$R_{y_0y_0}(t,t+\tau,\xi) = \int_{-\infty}^{\infty}\int_{-\infty}^{\infty} A(t+\tau,\omega) \cdot A(t,\omega) \cdot e^{i[\omega\tau+\kappa\xi]} \cdot f(\omega,\kappa)d\omega d\kappa \tag{96}$$

Concentrating now on the homogeneous, non-stationary stochastic wave $y_0(t,x)$, whose spectral and correlational characteristics are described by Eqs. 95 and 96, assume that $f(\omega,\kappa)$ is in the following form in order to account for possible dispersion:

$$f(\omega,\kappa) = f(\kappa) \cdot \delta[\omega - g(\kappa)] \tag{97}$$

where $\delta(\cdot)$ is Dirac's delta function and $g(\kappa)$ is a known function of κ. In this case, the simulation of the stochastic wave is performed using the following expression:

$$y(t,x) = \sqrt{2}\sum_{\ell=1}^{N} \sqrt{2A[t,g(\kappa_\ell)]^2 f(\kappa_\ell)\Delta\kappa} \cdot \cos[g(\kappa_\ell)t + \kappa_\ell x + \phi_\ell] \tag{98}$$

It will be shown now that the autocorrelation function of the simulated stochastic wave (by Eq. 98) is the same with the target autocorrelation function given by Eq. 96.

$$R_{yy}(t,t+\tau,x,x+\xi) = E\{y(t,x)y(t+\tau,x+\xi)\} =$$

$$= E\{\sqrt{2}\sum_{\ell=1}^{N}\sqrt{2A[t,g(\kappa_\ell)]^2 \cdot f(\kappa_\ell)\Delta\kappa}\cdot\cos[g(\kappa_\ell)t + \kappa_\ell x + \phi_\ell]\cdot$$

$$\cdot\sqrt{2}\sum_{m=1}^{N}\sqrt{2A[t+\tau,g(\kappa_m)]^2 \cdot f(\kappa_m)\Delta\kappa}\cdot$$

$$\cdot\cos[g(\kappa_m)\cdot(t+\tau) + \kappa_m(x+\xi) + \phi_m]\} =$$

$$= 2\sum_{\ell=1}^{N}\sum_{m=1}^{N}2A[t,g(\kappa_\ell)]\cdot A[t+\tau,g(\kappa_m)]\cdot\sqrt{f(\kappa_\ell)\cdot f(\kappa_m)}\cdot\Delta\kappa\cdot$$

$$\cdot E\{\cos[g(\kappa_\ell)t + \kappa_\ell x + \phi_\ell]\cdot\cos[g(\kappa_m)\cdot(t+\tau) + \kappa_m(x+\xi) + \phi_m]\} \qquad (99)$$

It can be easily shown again that the expectation appearing in Eq. 99 is different from zero only for $\ell=m$. Taking this into account, Eq. 99 becomes:

$$\sum_{\ell=1}^{N}2A[t,g(\kappa_\ell)]\cdot A[t+\tau,g(\kappa_\ell)]\cdot f(\kappa_\ell)\Delta\kappa\cdot\cos[g(\kappa_\ell)\tau + \kappa_\ell\xi] \qquad (100)$$

In the limit as $N \to \infty$ and with the value of κ_u fixed, the preceding equation can be written as:

$$\int_0^{\infty}2A[t,g(\kappa)]\cdot A[t+\tau,g(\kappa)]\cdot f(\kappa)\cdot\cos[g(\kappa)\tau + \kappa\xi]d\kappa \qquad (101)$$

Under the assumption that the integrand in Eq. 101 is an even function of κ, Eq. 101 yields:

$$R_{yy}(t,t+\tau,x,x+\xi) =$$

$$= \int_{-\infty}^{\infty} A[t,g(\kappa)] \cdot A[t+\tau,g(\kappa)] \cdot e^{i[g(\kappa)\tau+\kappa\xi]} f(\kappa)d\kappa =$$

$$= \int_{-\infty}^{\infty}\int_{-\infty}^{\infty} A[t,\omega] \cdot A[t+\tau,\omega] \cdot e^{i[\omega\tau+\kappa\xi]} \cdot f(\kappa) \cdot \delta[\omega - g(\kappa)]d\omega d\kappa =$$

$$= \int_{-\infty}^{\infty}\int_{-\infty}^{\infty} A(t,\omega) \cdot A(t+\tau,\omega) \cdot e^{i(\omega\tau+\kappa\xi)} \cdot f(\kappa,\omega)d\omega d\kappa =$$

$$= R_{yy}(t,t+\tau,\xi) = R_{y_0y_0}(t,t+\tau,\xi) \tag{102}$$

4.3 Numerical Example Involving a Non-Stationary Stochastic Wave With Two-Dimensional Spatial Nonhomogeneity

The evolutionary power spectrum of a non-stationary stochastic wave with two-dimensional spatial nonhomogeneity, is given by:

$$f(t,x_1,\omega,\kappa_1,\kappa_2)d\omega d\kappa_1 d\kappa_2 = \left|A(t,x_1,\omega,\kappa_1)\right|^2 \cdot f(\omega,\kappa_1,\kappa_2)d\omega d\kappa_1 d\kappa_2 \tag{103}$$

For the numerical example considered in this section, the modulating function $A(t,x_1,\omega,\kappa_1)$ is assumed to be of the form:

$$A(t,x_1,\omega,\kappa_1) = A(t,x_1,\omega) = B(t,\omega) \cdot W(t,x_1) \tag{104}$$

$B(t,\omega)$ describes the non-stationarity of the wave and is given by:

$$B(t,\omega) = \frac{\exp[-0.25t] - \exp[-(0.3765\cdot\omega + 0.251)\cdot t]}{\exp[-0.25t^*] - \exp[-(0.3765\cdot\omega + 0.251)\cdot t^*]} \tag{105}$$

and t^* indicates the time instant at which $B(t,\omega)$ assumes a maximum value as a function of t:

$$t^* = \frac{\ell n[0.3765 \cdot \omega + 0.251] - \ell n[0.25]}{0.3765 \cdot \omega + 0.001} \tag{106}$$

The plot of $B(t,\omega)$ as a function of t and ω is shown in Fig. 1, whereas $W(t,x_1)$ describes the nonhomogeneity of the wave and is given by:

$$W(t,x_1) = \begin{cases} 0 & \text{for } x_1 < x_T \\ \dfrac{x_1 - x_T}{x_L} & \text{for } x_T \leq x_1 \leq x_T + x_L \\ 1 & \text{for } x_1 > x_T + x_L \end{cases} \tag{107}$$

where

$$x_T = x_B - U_T \cdot t \tag{108}$$

The following values are used for x_L, x_B and U_T appearing in Eqs. 107 and 108:

$$x_L = 1{,}000 \text{ m} \; ; \qquad x_B = 6{,}000 \text{ m} \; ; \qquad U_T = 2{,}000 \frac{\text{m}}{\text{sec}} \tag{109}$$

The plot of $W(t,x_1)$ as a function of t and x_1 is shown in Fig. 2. The form of $f(\omega,\kappa_1,\kappa_2)$ is further assumed to be:

$$f(\omega,\kappa_1,\kappa_2) = f(\kappa_1,\kappa_2) \cdot \delta[\omega - g(\kappa_1,\kappa_2)] \tag{110}$$

where $f(\kappa_1,\kappa_2)$ is set to be:

$$f(\kappa_1,\kappa_2) = \frac{\sigma_{YY}^2}{8\pi} \cdot b_1^3 \cdot b_2 \cdot \kappa_1^2 \cdot \exp\left[-\left(\frac{b_1\kappa_1}{2}\right)^2 - \left(\frac{b_2\kappa_2}{2}\right)^2\right] \tag{111}$$

The power spectrum shown in Eq. 111 is proposed by Shinozuka and Harada[28] and based on data from the original accelerograms recorded on January 29, 1981 (Event 5) by a SMART-1 seismograph array installed at Lotung, Taiwan. The data represent the horizontal component of the displacement time history in the direction N13°W which is approximately the direction of the seismic source of this earthquake and are computed at each accelerogram station from two-

component data (EW & NS). The following values are used for σ_{yy}, b_1 and b_2 appearing in Eq. 111:

$$\sigma_{yy} = 0.0124 \text{ m}; \qquad b_1 = 1131 \text{ m}; \qquad b_2 = 3012 \text{ m} \tag{112}$$

The plot of $f(\kappa_1,\kappa_2)$ as a function of κ_1 and κ_2 is shown in Fig. 3. Solely for the purpose of numerical demonstration, function $g(\kappa_1,\kappa_2)$ is assumed to be of the form:

$$g(\kappa_1,\kappa_2) = c \cdot \sqrt{\kappa_1^2 + \kappa_2^2} \tag{113}$$

in which the value of the phase velocity c is assumed to be:

$$c = 2{,}800 \text{ m/sec} \tag{114}$$

Finally, the stochastic wave $y(t,x_1,x_2)$ can be simulated using the following expression and under the assumption of quadrant symmetry in terms of the space variables x_1 and x_2:

$$y(t,x_1,x_2) = \sqrt{2} \sum_{\ell_1=1}^{N_1} \sum_{\ell_2=1}^{N_2} \sqrt{2A[t,x_1,g(\kappa_{1\ell_1},\kappa_{2\ell_2})]^2 \cdot f(\kappa_{1\ell_1},\kappa_{2\ell_2})} \cdot$$

$$\cdot \sqrt{\Delta\kappa_1 \Delta\kappa_2} \cdot \{\cos[g(\kappa_{1\ell_1},\kappa_{2\ell_2})t + \kappa_{1\ell_1}x_1 + \kappa_{2\ell_2}x_2 + \phi^{(1)}_{\ell_1\ell_2}] +$$

$$+ \cos[g(\kappa_{1\ell_1},\kappa_{2\ell_2})t + \kappa_{1\ell_1}x_1 - \kappa_{2\ell_2}x_2 + \phi^{(2)}_{\ell_1\ell_2}]\} \tag{115}$$

where:

$$\Delta\kappa_1 = \frac{\kappa_{1u}}{N_1}\ ; \qquad \Delta\kappa_2 = \frac{\kappa_{2u}}{N_2} \tag{116}$$

$$\kappa_{1\ell_1} = \ell_1 \cdot \Delta\kappa_1\ ; \qquad \ell_1 = 1,2,\ldots,N_1 \tag{117}$$

$$\kappa_{2\ell_2} = \ell_2 \cdot \Delta\kappa_2 \; ; \qquad \ell_2 = 1,2,\ldots,N_2 \tag{118}$$

The following values are used for N_1, N_2, κ_{1u} and κ_{2u}:

$$N_1 = N_2 = 64 \tag{119}$$

$$\kappa_{1u} = 8.84 \times 10^{-3} \text{ rad/m}; \qquad \kappa_{2u} = 3.32 \times 10^{-3} \text{ rad/m} \tag{120}$$

It is noted again that $\phi^{(1)}_{\ell_1\ell_2}$ and $\phi^{(2)}_{\ell_1\ell_2}$ are two sequences of independent random phase angles uniformly distributed in the range $(0,2\pi)$.

The stochastic wave is now simulated, using Eq. 115, over a 10,000 m x 10,000 m area. The simulation is performed at 12 equispaced time instants, 0.5 sec apart from each other, and shown in Fig. 4. It is clearly observed in all twelve plots that there is relatively rapid variation along the x_1-axis (which represents the major axis of seismic wave propagation in Event 5) compared to the variation along the x_2-axis. From the number of peaks (4) along the x_1-axis, the apparent wave length along this axis is estimated to be around 2,500 m. Thus, the patterns shown in Fig. 4 indicate a dominant wave with a wave length of approximately 2,500 m propagating in the negative x_1-direction. By dividing the distance covered by a single peak (5,500 m) by the elapsed time (2.0 sec), the approximate speed of wave propagation along the x_1-axis is estimated to be 2,750 m/sec. This value is practically identical to the value of 2,800 m/sec specified in Eq. 114. These wave length and phase velocity values result in a dominant frequency of approximately $2,800/2500 \doteq 1.12$ Hz. This is also confirmed by Fig. 5 which plots the time history of the displacement at x_1 = 3,500 m and x_2 = 1,000 m (point A in Fig. 4a). The apparent frequency observed in this plot is 1/0.75 sec = 1.33 Hz, which is very close to the above-mentioned dominant frequency of 1.12 Hz. The time histories at points B, C and D (also shown in Fig. 4a) are also plotted in Fig.

5. The time histories at A, B and C show the spatial variability along the major axis of wave propagation while those at A and D along the direction perpendicular to that. The propagating wave front is clearly seen in Fig. 4b as well as in the first three frames of Fig. 5 (points A, B and C). The ground is at rest in front of the wave front because of Eq. 107. Another interesting feature that can be observed in Fig. 4 is the initial gradual increase of the amplitude of the wave and the subsequent gradual decrease which is an actual feature of all strong ground motions. At this point, it is pointed out that the same procedure as the one described above for the digital simulation of the displacement time history can be used for the digital simulation of either the velocity or acceleration time history, by properly choosing the corresponding evolutionary power spectra.

Finally, it is noted that the CPU time necessary to generate 21x21 points at a specific time instant was approximately 11 minutes (on a SUN 3/180 computer system).

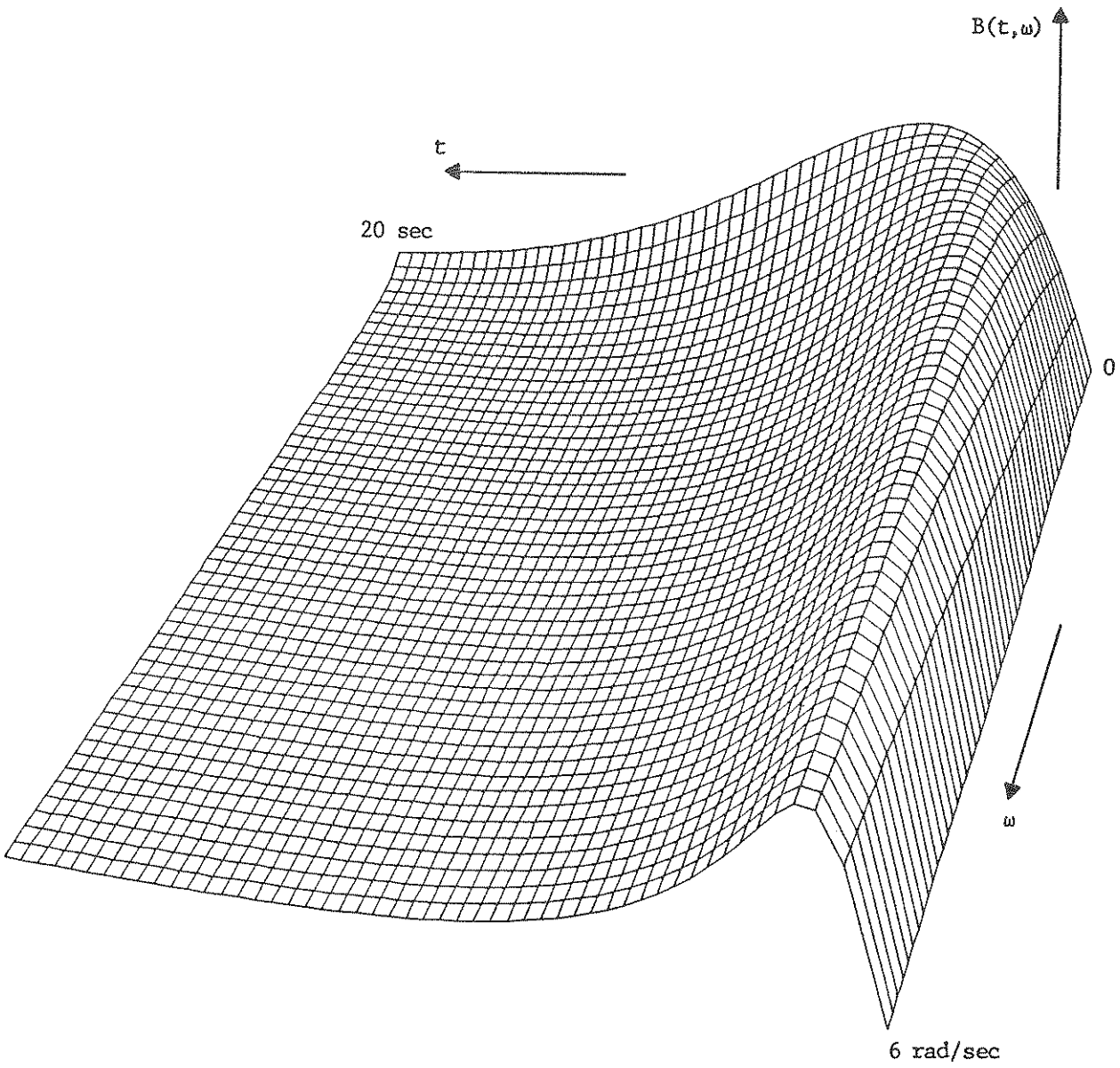

Fig. 1 Function $B(t,\omega)$.

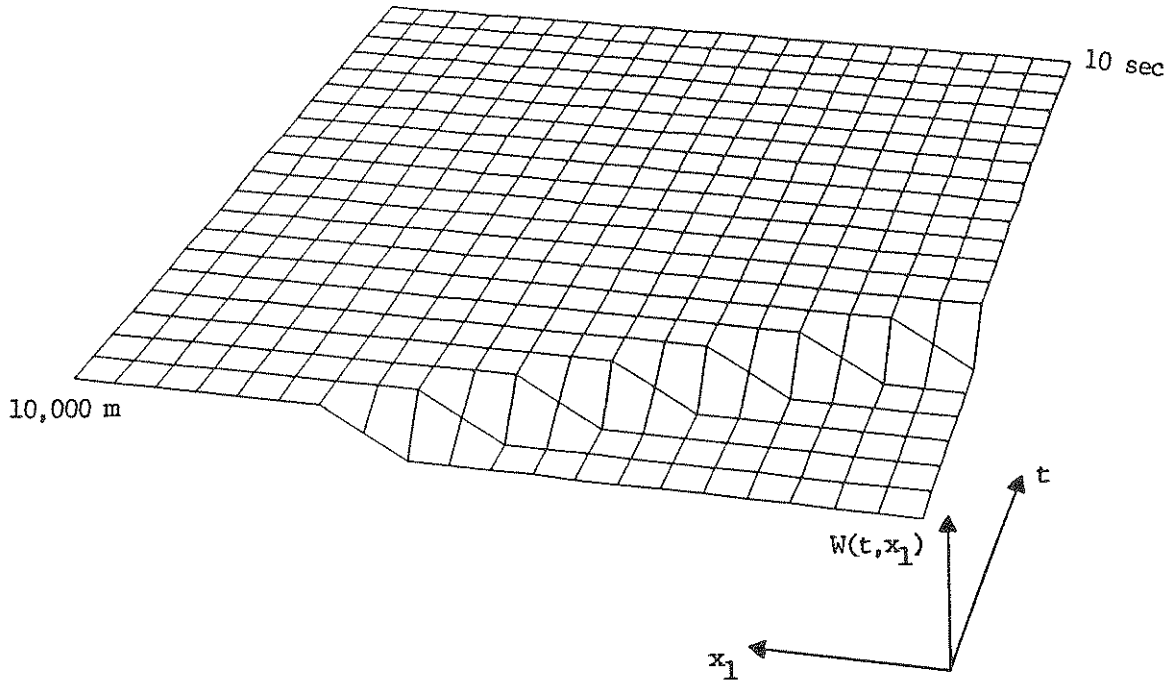

Fig. 2 Function $W(t, x_1)$.

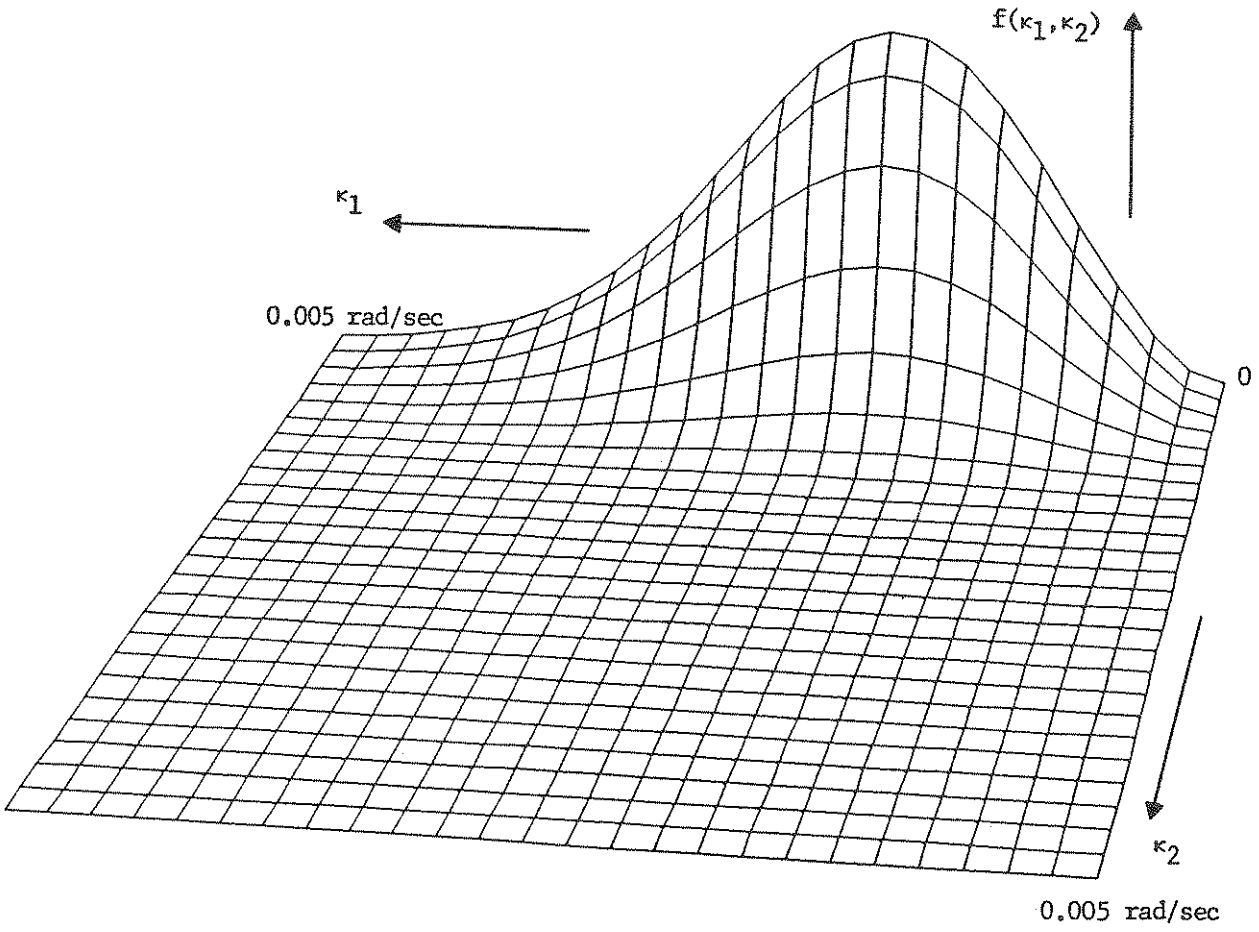

Fig. 3 Power Spectrum $f(\kappa_1, \kappa_2)$.

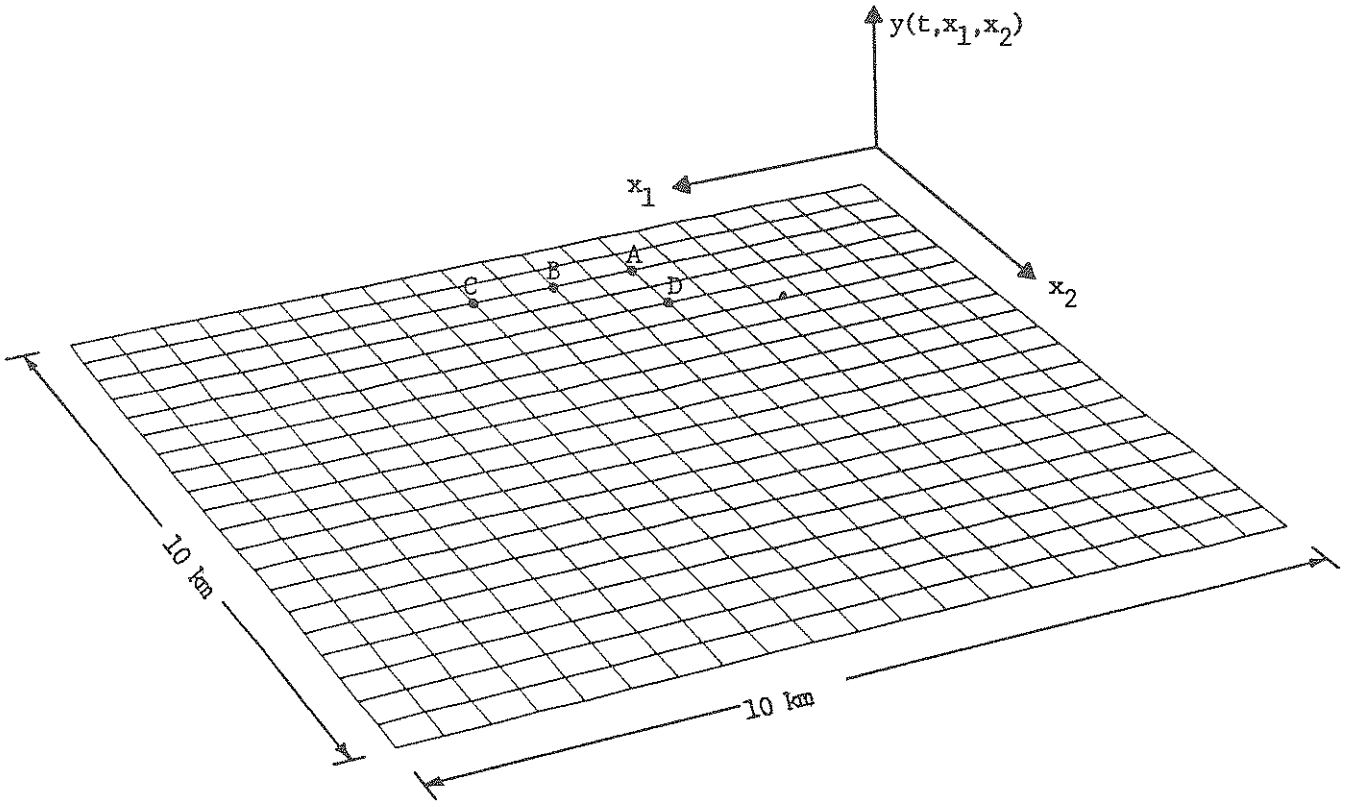

Fig. 4a Simulated Stochastic Wave at 12 Equispaced Time Instants (configuration of simulated points).

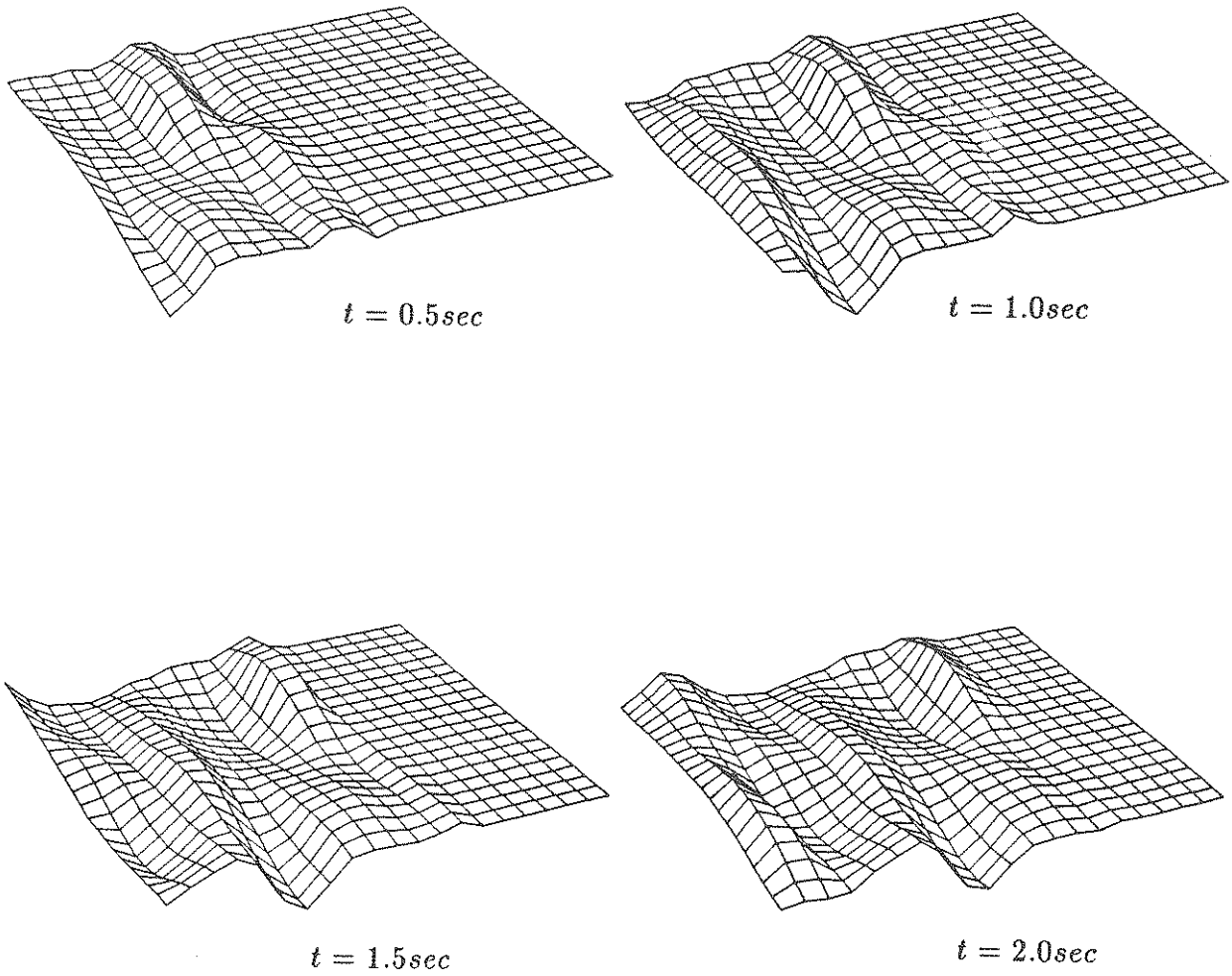

Fig. 4b Simulated Stochastic Wave at 12 Equispaced Time Instants.

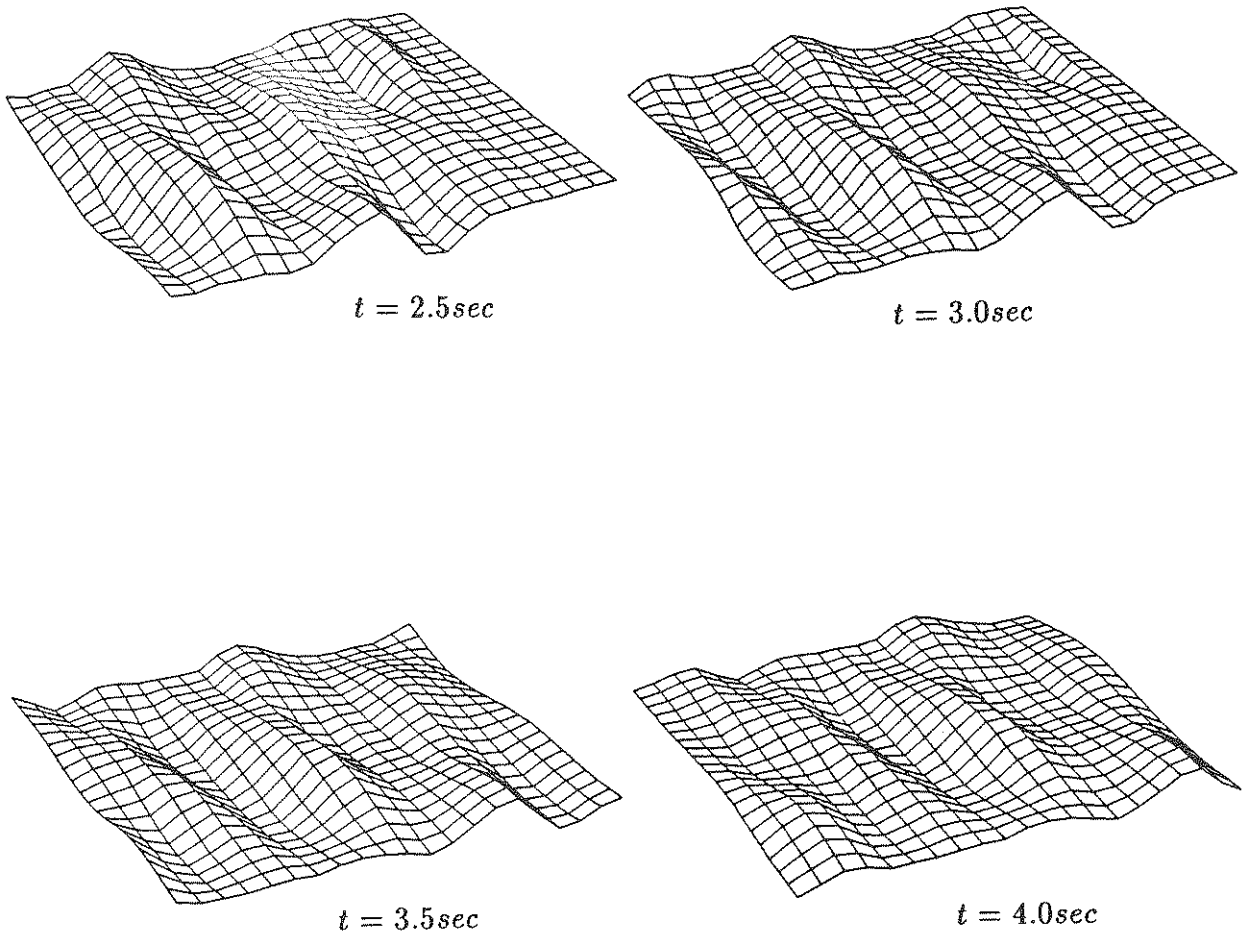

Fig. 4c Simulated Stochastic Wave at 12 Equispaced Time Instants.

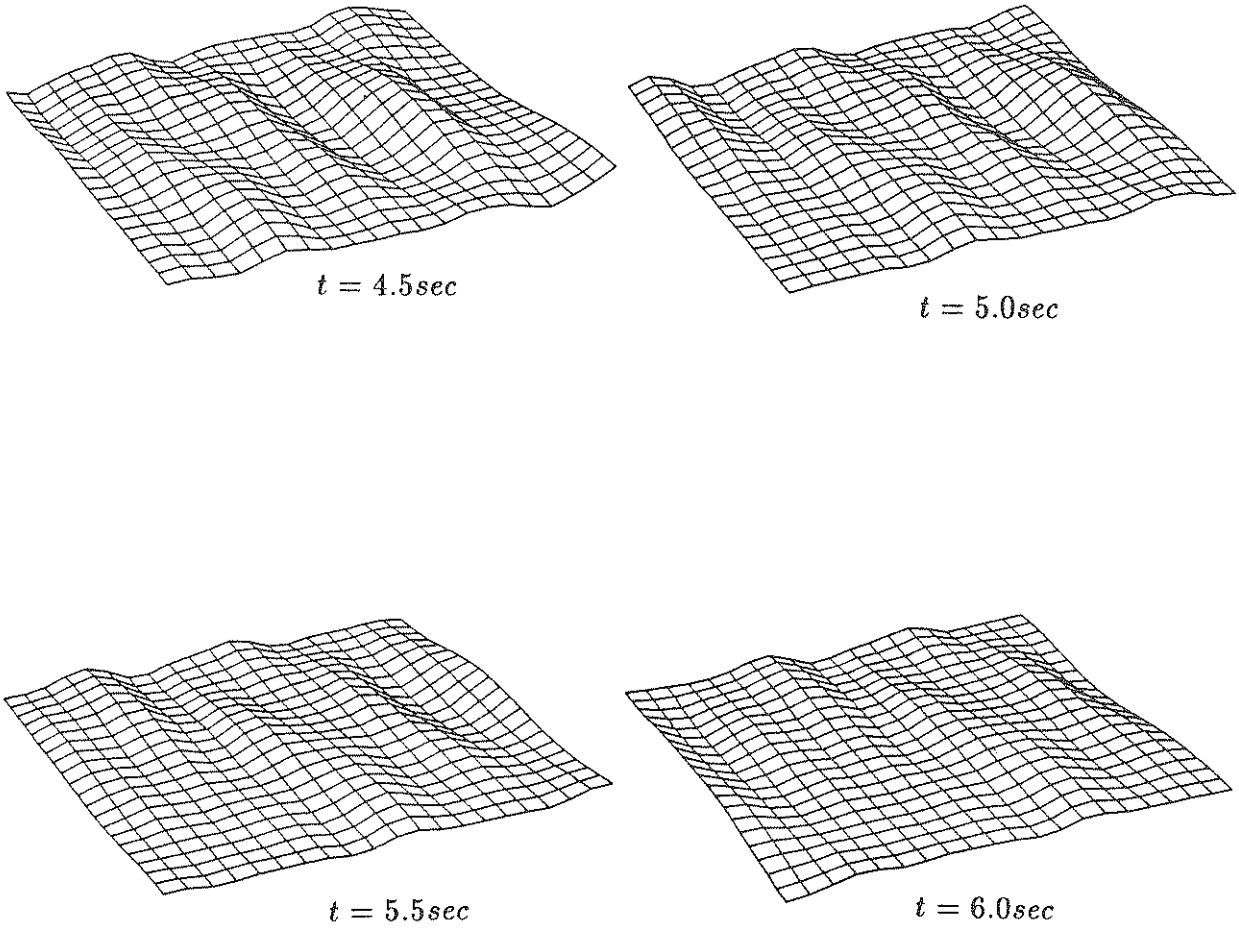

Fig. 4d Simulated Stochastic Wave at 12 Equispaced Time Instants.

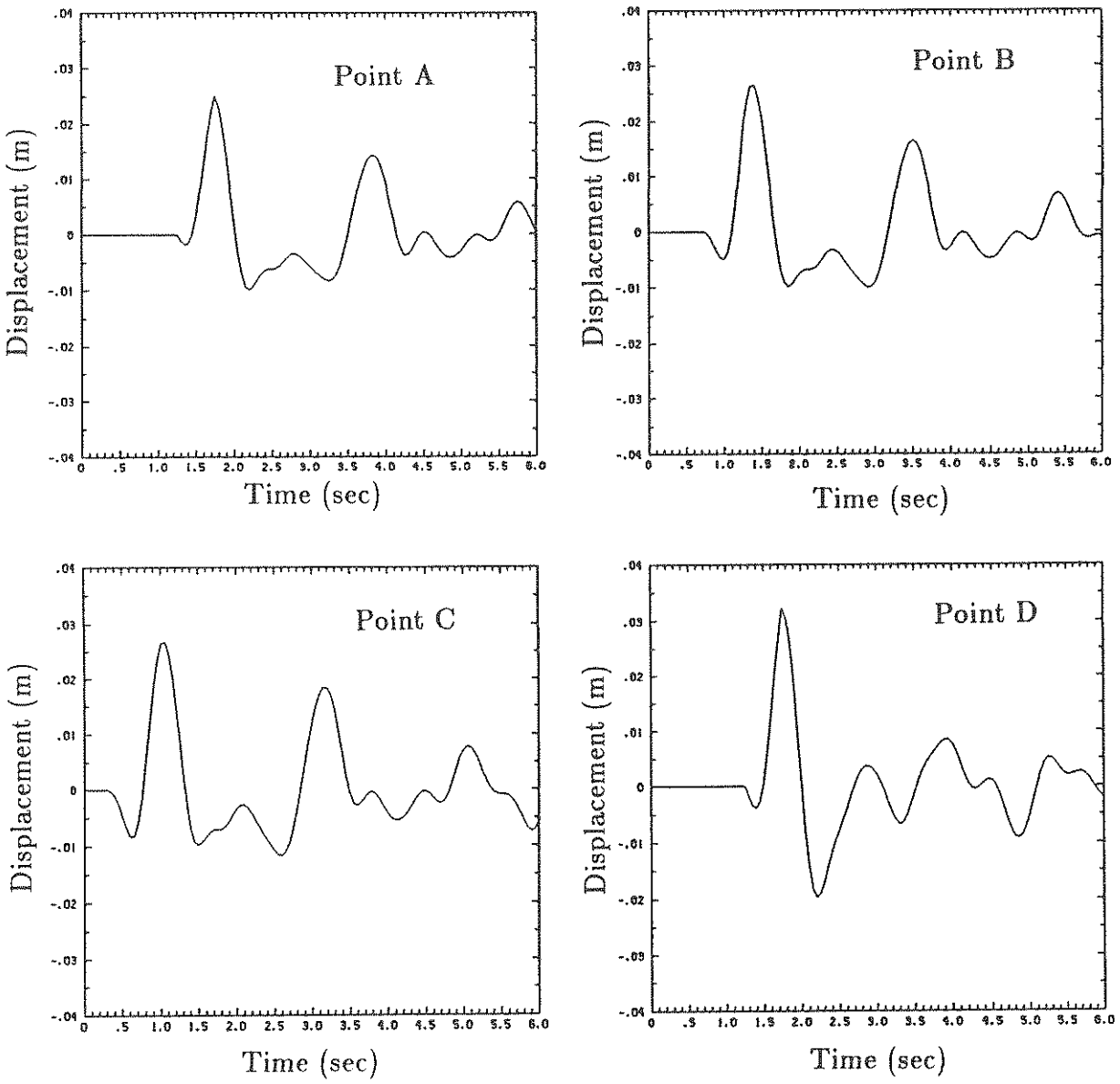

Fig. 5 Time History of Displacement at the Four Points A, B, C and D shown in Fig. 4a.

5. CONCLUSION

This paper presented fundamentals of the theory of multi-dimensional and multi-variate stochastic fields and stochastic waves. This was done primarily from the viewpoint of applying it to the digital generation of seismic ground motion for the purpose of seismic response analysis of lifeline systems extending over a large spatial area. The method appears to work very well, as exemplified by a numerical example where a propagating seismic wave idealized as a spatially two-dimensional stochastic wave is digitally generated.

While such results are gratifying, there appear to be some issues that still need to be resolved by future study. For example, the spectral representation used in this paper produces mathematical models for stochastic processes, fields and waves which are asymptotically Gaussian. However, Gaussianess may not always apply to the actual ground motion data. If the data exhibit some deviation from Gaussianess, and such deviation is expected to substantially affect the result of the ensuing analysis, then non-Gaussian characteristics must be introduced into the model. In this respect, a recent work by Yamazaki and Shinozuka[29] may prove to be quite useful, because the paper[29] deals with multi-dimensional stochastic fields and introduces non-Gaussian characteristics still on the basis of spectral representation. An alternative consists of the use of shot noise or filtered Poisson process models, as demonstrated by Lin[8] and Shinozuka and Sato[4]. More recently, Lin[30] showed how the evolutionary power spectrum can be incorporated into the filtered Poisson model. However, these filtered Poisson models are limited to one-dimensional and uni-variate cases at this time.

Another issue that requires further study is the question of how more general dispersion characteristics can be incorporated into the model. In the present formulation, a particular relationship is assumed for the frequency

and wave numbers. In this connection, if a number of seismic waves of specific characteristics are known to be propagating simultaneously, the spectral representation of these models can be constructed individually and summed up vectorially to develop a simulation of such a composite wave. Since, however, the observed ground motion is a composite of seismic waves with various characteristics, no simple relationship can really be assigned to the frequency and wave number. It is therefore reasonable to assume that a multiplicity of such relationships exist in reality and, indeed, the power spectral density obtained from ground motion data involving the frequency and all pertinent wave numbers should contain information relevant to this. It is important and also interesting to pursue this issue. It should be noted that Scherer and Schueller have done some interesting work in this area[31].

Another aspect of future work is the extension of the introduced simulation technique to multi-variate non-stationary and/or nonhomogeneous cases of stochastic waves. However, such a task might be particularly difficult, because the cross-correlational characteristics of such waves are usually very complicated and no reliable data are available at this time for non-stationary and/or nonhomogeneous multi-variate stochastic waves.

The simulation of ground motion described in this paper represents, in essence, mathematically tractable and physically meaningful models. Indeed, we have come a long way from the early mathematical model in which a Gaussian white noise is passed through an appropriate filter by means of a convolution integral to produce 1D-1V artificial ground accelerations. While some attempt has been made in this paper to incorporate into the models the physical laws of propagating seismic waves, further efforts should be directed to the improvement of these models so as to reflect the physics of seismic waves including their source mechanism, attenuation, etc.

Finally, the following problem is currently under investigation: given the evolutionary power spectrum of a spatially two-dimensional, nonhomogeneous, non-stationary stochastic wave (shown in Eq. 103), derive the corresponding evolutionary power spectrum of the non-stationary stochastic process obtained by freezing the space variables x_1 and x_2 at a specific point. Clarification of the above issue will provide further insight into the theory of stochastic waves.

ACKNOWLEDGEMENT

This work was supported by Sub-contract No. SUNYRF-NCEER-86-3043 under the auspices of the National Center for Earthquake Engineering Research under NSF Grant No. ECE-86-07591.

REFERENCES

1. Tajimi, H., "Basic Theories on Aseismic Design of Structures," Institute of Industrial Science, University of Tokyo, Vol. 8, No. 4, March 1959.

2. Cornell, C.A., "Stochastic Process Models in Structural Engineering," Technical Report No. 34, Dept. of Civil Engineering, Stanford University, May 1960.

3. Housner, G.W. and Jennings, P.C., "Generation of Artificial Earthquakes," Journal of Engineering Mechanics, ASCE, Vol. 90, No. EM1, February 1964, pp. 113-150.

4. Shinozuka, M. and Sato, Y., "Simulation of Nonstationary Random Process," Journal of Engineering Mechanics ASCE, Vol. 93, No. EM1, February 1967, pp. 11-40.

5. Amin, M. and Ang, A.H-S., "Nonstationary Stochastic Models of Earthquake," Journal of Engineering Mechanics, ASCE, Vol. 94, No. EM2, April 1968, pp. 559-583.

6. Iyengar, R.N. and Iyengar, K.T.S., "A Nonstationary Random Process Model for Earthquake Accelerograms," Bulletin of the Seismological Society of America, Vol. 59, No. 3, June 1969, pp. 1163-1188.

7. Ruiz, P. and Penzien, J., "Stochastic Seismic Response of Structures," Journal of Engineering Mechanics, ASCE, Vol. 97, No. EM2, April 1971, pp. 441-456.

8. Lin, Y-K., "Nonstationary Excitation and Response Treated as Sequences of Random Pulses," Journal of the Acoustical Society of America, Vol. 38, 1965, pp. 453-460.

9. Shinozuka, M., "Monte Carlo Solution of Structural Dynamics," International Journal of Computers and Structures, Vol. 2, 1972, pp. 855-874.

10. Shinozuka, M. and Jan, C-M., "Digital Simulation of Random Processes and Its Applications," Journal of Sound and Vibration, Vol. 25, No. 1, 1972, pp. 111-128.

11. Iyengar, R.N. and Shinozuka, M., "Effect of Self-Weight and Vertical Acceleration on the Behavior of Tall Structures During Earthquake," Journal of Earthquake Engineering and Structural Dynamics, Vol. 1, 1972, pp. 69-78.

12. Shinozuka, M., "Digital Simulation of Ground Acceleration," Proceedings of the 5th World Conference on Earthquake Engineering, Rome, Italy, June 1973, pp. 2829-2838.

13. Shinozuka, M., "Digital Simulation of Random Processes in Engineering Mechanics with the Aid of FFT Technique," Stochastic Problems in Mechanics, Eds. S.T. Ariaratnam ane H.H.E. Leipholz, (Waterloo: University of Waterloo Press), 1974, pp. 277-286.

14. Shinozuka, M., "Stochastic Fields and Their Digital Simulation," Lecture Notes for the CISM Course on Stochastic Methods in Structural Mechanics, Udine, Italy, August 28-30, 1985.

15. Samaras, E.F., Shinozuka, M. and Tsurui, A., "ARMA Representation of Random Vector Processes," Journal of Engineering Mechanics, ASCE, Vol. 111, No. 3, pp.449-461.

16. Naganuma, T. et al., "Digital Generation of Multidimensional Random Fields," Proceedings of ICOSSAR '85, Kobe, Japan, May 27-29, 1985, pp. I.251 - I.260.

17. Naganuma, T., Deodatis, G. and Shinozuka, M., "ARMA Model for Two-Dimensional Processes," Journal of Engineering Mechanics, ASCE, Vol. 113, No. 2, February 1987, pp. 234-251.

18. Deodatis, G., Shinozuka, M. and Samaras, E., "An AR Model for Non-Stationary Processes," Proceedings of the 2nd International Conference on Soil Dynamics and Earthquake Engineering, on board the liner Queen Elizabeth 2, New York to Southampton, June/July 1985, pp. 2.57 - 2.66.

19. Deodatis, G. and Shinozuka, M., "An Auto-Regressive Model for Non-Stationary Stochastic Processes," accepted for publication in the ASCE Journal of Engineering Mechanics.

20. Spanos, P.D. and Hansen, J., "Linear Prediction Theory for Digital Simulations of Sea Waves," Journal of Energy Resources Technology, ASME, Vol. 103, 1981, pp. 243-249.

21. Spanos, P.D., "ARMA Algorithms for Ocean Spectral Modeling," Journal of Energy Resources Technology, Vol. 105, 1983, pp. 300-309.

22. Spanos, P.D. and Solomos, G.P., "Markov Approximation to Nonstationary Random Vibration," Journal of Engineering Mechanics, ASCE, Vol. 109, No. 4, 1983, pp. 1134-1150.

23. Kozin, F. and Nakajima, F., "The Order Determination Problem for Linear Time-Varying AR Models," IEEE Transactions on Automatic Control, Vol. AC-25, No. 2, 1980, pp. 250-257.

24. Vanmarcke, E., Random Fields, (Cambridge: MIT Press), 1984.

25. Priestley, M.B., "Evolutionary Spectra and Non-Stationary Processes," Journal of the Royal Statistical Society, Series B., Vol. 27, 1965, pp. 204-237.

26. Priestley, M.B., "Power Spectral Analysis of Non-Stationary Random Processes," Journal of Sound and Vibration, Vol. 6, No. 1, 1967, pp. 86-97.

27. Liu, S-C., "Evolutionary Power Spectral Density of Strong Motion Earthquakes," Bulletin of the Seismological Society of America, Vol. 60, No. 3, 1970, pp. 891-900.

28. Shinozuka, M. and Harada, T., "Harmonic Analysis and Simulation of Homo-

geneous Stochastic Fields," Technical Report, Department of Civil Engineering and Engineering Mechanics, Columbia University, New York, 1986.

29. Yamazaki, F. and Shinozuka, M., "Digital Generation of Non-Gaussian Stochastic Fields," Technical Report, Department of Civil Engineering and Engineering Mechanics, Columbia University, New York, 1986.

30. Lin, Y-K., "On Random Pulse Train and Its Evolutionary Spectral Representation," Journal of Probabilistic Engineering Mechanics, Vol. 1, No. 4, December 1986, pp. 219-223.

31. Scherer, R.J. and Schueller, G.I., "The Acceleration Spectrum at the Base Rock Determined From a Non-Stationary Stochastic Source Model," Proceedings of the 8th European Conference on Earthquake Engineering, Portugal, Vol. 1, 1986, pp. 3.3/47 - 3.3/54.